CHAPTER-II

CHAPTER - II

THEORETICAL BACKGROUND.

2.1 Introduction .

The emerging technology of modern days needs various types of thin films for a variety of applications |32, 33|. The thin films can be single or multicomponent, alloy/compound or multilayer coating on substrates of different shapes and sizes |34-36 . The properties required of the films can be depending on the applications, high optical reflection/transmission hardness, wear resistances, single crystal nature etc. Such a versatility in thin films is brought about by the techniques of thin film deposition |35-40|.

Although the thin films are assuming increasingly interest, their structure is complex in view of their applications which demand taylor-made properties. As a result, sophisticated characterisation techniques have emerged out for understanding of the multifarious properties of thin films. Depending on the property of interest, a host of characterisation tools are available for giving some times similar and more often additional and complementary informations. No one technique is sufficient to characterise a thin film completely even in any one domain such as crystal structure, chemical and physical nature etc. The properties relevant for thin film studies and corresponding characterisation methods are so many in numbers that it is impossible to cover all aspects in any one of the review.

Further, film properties are the strong function of deposition technique and it is quite obvious that no one technique can deposit the films covering all beneficial aspects such as temperature, cost of the equipments, deposition conditions and parameters and other selective properties of the films.

2.2 Survey of Thin Film Deposition Techniques.

As is mentioned above, the properties required of the films can be depending upon the applications and multifarious characterisation techniques, a versatility in thin films is brought about by techniques of thin film deposition. The basic steps involved in a thin film deposition technique are :

a) Creation of material(s) to be deposited in an atomic, molecular or particulate forms prior to the deposition.

b) Transport of material(s) thus, created to the substrate in the form of a vapour stream or solid or spray etc.

c) Deposition of the material(s) on the substrate and film growth by a nucleation and growth process.

All the deposition techniques can be distinguished by the way the three basic steps above are effected. One can in principle get films of desired properties by properly modifying these three steps.

Thin film deposition techniques have been broadly classified in four main categories;

1) Physical Vapour Depositions (PVD).
2) Chemical Vapour Depositions (CVD).
3) Electroless or Solution Growth Deposition.
4) Electrochemical Deposition (ECD).

2.2.1 Physical vapour depositions (PVD).

The Physical Vapour Deposition techniques are those in which the material to be deposited is made available in an atomic, molecular or particulate form before being put for deposition. The PVD's can further be subdivided into:

i) Thermal Evaporation (T.E.),
ii) Electron Beam Evaporation (EBE),
iii) Molecular Beam Epitaxy (MBE),
iv) Activated Reactive Evaporation (ARE) and
v) Ion Plating.

The first three techniques are different in the way the vapour beam is created (step a). In ARE, step-b is modified in that the vapour beam is transported through a reactive plasma. In ion plating, conditions at the substrates (step-c) are modified by an ion beam. The major advantage of using PVD techniques is that all the three deposition steps (step a,b,c) can be independently controlled. However, this spells out a warning that the deposition parameters should be carefully monitored in order to achieve reproducible films. The details of all the PVD techniques is beyond the aim of this dissertation and reader may refer to referances 1 to 6.

2.2.2 Chemical deposition techniques.

Chemical deposition techniques are the most important tools for the growth of thin films owing to their versatility for depositing a very large number of elements and compounds at relatively low temperature |41|. Both in the form of vitreous and crystalline layers , with high degree of perfection and purity, these films can be deposited with required stoichiometry. Large or small and even or uneven surfaces of all types, conducting or insulating can be coated with relative ease. The processes are very economical and have been industrially exploited to large scale. The various chemical deposition processes are as follows:

1) Chemical Vapour Deposition (CVD).
2) Spray Pyrolysis.
3) Electrodeposition.
4) Anodization.
5) Screen Printing.
6) Solution Growth.

A detailed history of each of above technique is not possible to mention here, however, a brief idea is explained for the sake of understanding.

1) Chemical Vapour Deposition (CVD).

A simple definition of CVD is the condensation of a compound or compounds from the gas phase onto a substrate where reaction occurs to produce a solid deposit. A liquid or solid compound to be deposited is made gaseous by volatilization and is caused to flow either by a pressure differential or by the carrier gas to the substrate. The chemical reaction is initiated at or near the substrate surface to produce the desired deposit on the substrate. In some processes the chemical reaction may be activated through an external agency such as heat, R.F.field, light, X-rays, electric field or glow discharge, electron bombardment etc. The morphology microstructure and adhesion of the deposit is a strong function of the nature of the reaction and the activation process . The possible reactions involved in CVD are: thermal decomposition, hydrogen reductiion,nitridation, carbidization or oxidation, disproportionation, chemical transport reactions and combined reactions. In most reactions, the deposition is heterogeneous in character. Homogeneous reaction may occur in gas phase resulting in undesirable powdery or flaky deposits.

The feasibility of CVD process can be predicted by studying the thermodynamics of the reactions. The reaction kinetics and mechanism of film growth are so different in individual processes, that a generalised account is not possible. However, certain important features common to all these methods are : 1) CVD set-ups are simple and fast recycle times are possible, ii) high deposition rates are achieved, iii) Deposition of the compounds and multicomponent alloys and control of their stoichiometry is possible, iv) Epitaxial layer of high perfection and low impurity content can be grown, v) Objects of complex shapes and geometries can be coated and vi) In-situ chemical vapour etching of the substrates prior to deposition is possible. The factors which are uncommon and affect the deposition, uniformity, composition and properties of film are :

i) Thermodynamics and reaction kinetics involved in the deposition process are very complex and poorly understood.

ii) Higher substrate temperatures are required as compared to PVD processes.

iii) Highly toxic sometimes explosive and corrosive gases and volatile products are involved in the reactions. These may attack the substrate deposit and the chamber walls.

iv) High temperature in the process lead to diffusion, alloying or to a limited choice of the substrate materials.

v) Uniformity of the deposit and masking of the substrates is usually difficult.

2) Spray pyrolysis :

This is essentially a thermally stimulated reaction between clusters of liquid/vapour atoms of different spraying solution of the desired compound on to a substrate maintained at evelated temperatures. The sprayed droplets on reaching the hot substrate undergo pyrolytic decomposition and form a single crystal or cluster of a crystallite of the product. The other volatile byproducts and excess solvents escape in the vapour phase. The thermal energy for decomposition, subsequent recombination of the species, sintering and recrystallisation of crystallite is provided by hot substrates. The nature of the fine spray droplets depend upon spray nozzle with the help of a carrier gas. The chemicals used for this method should be such that the desired thin film materials must be obtained as a result of thermally activated reaction between the different species and remainder of the chemical constituents. The carrier liquid/gas should be volatile at the deposition temperature. Growth of the film by spray pyrolysis is determined by nature of the substrate, chemical nature and concentration of the spray solution and spray parameters. The films are in general strong and adherent, mechanically hard, pinhole free and stable with time and temperature. The topography of the films is generally rough and dependent on spray conditions. The substrate surfaces get affected in the spray process and the choice is limited to glass, quartz, ceramics or oxide, nitride or carbide coated substrates. Metallic substrates found unsuitable for this process. Stoichiometry for oxides is difficult to maintain by this process.

3) Electrodeposition :

It is a process of depositing a substance upon an electrode by electrolysis, the chemical changes being brought about by the passage of a current through an electrolyte. The phenomenon of electrolysis is governed by the Faraday's laws. When a metal electrode is dipped in a solution containing ions of that metal, a dynamic equilibrium $M \rightleftharpoons M^{+x} + Xe$ (M-Metal atom) is set up. The electrode gains a certain charge on itself which attracts oppositely charged ions and molecules, holding them at the electrode/electrolyte interface. A double layer consisting of an inner layer of water molecules interposed by preferentially adsorbed ions and outer layer of the charge opposite to that of the electrode is formed. During deposition ions reach the electrode surface, stabilise on it, release their ligands (water molecules or complexing agent), release their charges and undergo electrochemical reaction. The rapid depletion of the depositing ions from the double layer is compensated by a continuous supply of fresh ions from the bulk of the electrolyte.The transport of ions to depletion region occurs due to the diffusion, owing to concentration gradient and migration owing to the applied electric field and convection currents. The factors influencing electrodeposition process are :

i) pH of the electrolyte, ii) current density, iii) temperature of the bath, iv) bath composition, v) electrode shape and vi) agitation.

4) Anodization .

It is an electrolytic process wherein the metal is made the anode in a suitable electrolyte. When an electric current is passed, the surface of the metal is converted into its oxide having decorative, protective or other properties. The cathode is metal or graphite where H_2 evolves. The required oxygen originates from the electrolyte used. The pH of the electrolyte plays an important part in obtaining the coherent films. Thickness of the oxide layer depends on the metal, voltage applied, temperature of the bath and time of deposition.

5) Screen Printing.

Screen printing is essentially a thick film process in which pastes containing the desired material are screen printed by conventional method onto a suitable substrate to define conductor, resistor or a device pattern. Subsequently, the substrate is fixed under appropriate conditions of time and temperature to yield rugged components bonded to the substrate. The substrates which have smooth surface, capability of withstanding for higher temperature, mechanical strength, high thermal conductivity and good electrical properties and are compatible with film material pastes are used (Alumina, beryllia, magnesia, thoria and Zirconia). The paste to be used normally consists of : i) a metallic/resistive/dielectric/semiconducting component in finely divided powder form, ii) bonding agent, iii) an organic suspension medium, and iv) an organic diluent. Semiconductors like CdTe,CdS,CdSe etc. can be deposited by this technique.

6) Solution Growth :

Films can be grown on either metallic or nonmetallic substrates by dipping them in appropriate solutions of metal salts without the application of any electric field. Deposition may occur by homogeneous chemical reactions usually reduction of metal ions in solution by a reducing agent. If this occur on a catalytic surface it is called an electroless deposition (autocatalytic). Silvering is the most widely used of this techniques. Metallic as well as compound films (sulphides, selenides) and their alloys can be deposited. For non-metallic surfaces a sensitizer has to be used. The rate of growth and degree of crystallinity depends upon the temperature of the solution. One of the chief advantages of such a method is to deposit the films on non accessible surface i.e inside of glass tubes etc.

2.3 Chemical Deposition Process And Mechanism of Bi_2S_3 Film Formation.

Brief Discussion of few of the different preparative methods of the polycrystalline materials is given in the previous section (section 2.2). This section describes the overriding advantages of a chemical deposition process used in these investigations and mechanism of the Bi_2S_3 film formation.

2.3.1 Advantages of a chemical deposition process | 39,43 | :

The chemical deposition pocess is adopted owing to :

i) The method does not require sophisticated instrumentation like vaccum system and other expensive equipments. It can be carried out in a glass beaker only; an oil bath and stirrer are the equipments needed and hence power consumption is also negligible. Further, it is cheap due to very small quantity of the active materials.

ii) The method is ideally suited for large area deposition; it can be done by using large volume vessels.

iii) A large number of substrates can be coated in a single run with a proper design. The design includes only positioning of the substrates along the wall of the reaction container.

iv) Electrical conductivity of the substrates is not a hard and fast requirement. Hence any insoluble surface to which the solution has free access will be a suitable substrate for deposition.

v) The deposition is at low temerature and avoids oxidation or corrosion of the metallic substrates. Further, the low temperature allows a differential crackfree deposits.

vi) The method yields pinhole free, uniform deposits as the solution from which the films are deposited, always remains in touch with substrates.

vii) Stoichiometric deposits can easily be obtained since the basic building blocks are ions instead of atoms.

viii) Doping of foreign impurity can easily be achieved.

ix) The process of film growth is slow which facilitates better orientation of crystallite with improved grain structure.

x) A provision for vigourous stirring of reaction solution is not needed. The substrate holder is designed such that substrates attached to it churn well the bulk of the mixture and each time the surface of the deposit is exposed to new building blocks of Bi^{3+} and S^{2-}.

xi) Compound films such as sulphides and selenides of Cd, Pb, Zn, and Hg and their alloys can be easily deposited.

xii) The important and cheap advantage of this method is that it is possible to deposit films on non-accessible surface i.e. inside of glass tubes etc., where they will be protected from physical damages. The detailed procedure followed during the work is summarised in the experimental part of this dissertation.

2.3.2 Mechanism of Bi_2S_3 film formation :

As discussed in section 2.3.1., the chemical deposition process for the deposition of thin films is relativly inexpensive, simple and convenient technique for the preparation of large area semiconducting materials especially of II - VI and IV - VI compounds and hybrids thereof. The method has several overriding advantages |39-43|. Using this popular technique thin films of bismuth trisulphide have been prepared onto the glass substrates by allowing them to remain in an aqueous solution of the reactants for a period equal to the deposition time. The bismuth nitrate was triturated with triethanolamine and a fixed quantity of Bi^{2+} triturated complex was allowed to react with appropriate solutions of thiourea and ammonium hydroxide and the resulting mixture was raised to about 95°C. The basic overall reaction can be given as |42-16| :

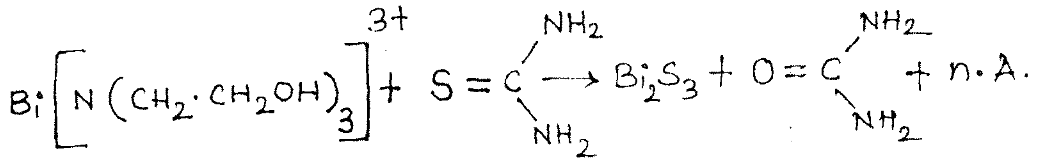

$$Bi\left[N(CH_2\cdot CH_2OH)_3\right]^{3+} + S=C\begin{matrix}NH_2\\ NH_2\end{matrix} \longrightarrow Bi_2S_3 + O=C\begin{matrix}NH_2\\ NH_2\end{matrix} + n\cdot A.$$

where, A = complexing agent, $N(CH_2CH_2OH)_3$.

The pH of the solution was maintained around 9.5. Thiourea is used for the slow release of S^{2-} ions. The NH_4OH is added to slow down the formation of Bi_2S_3 and to increase its adherence on the substrate material.

In chemical deposition process, the film forms slowly, which facilitates better orientation of crystallites with improved grain structure. Depending on the deposition conditions such as temperature of the mixture, stirring rate, pH of the solution, solution concentrations and its purity and quality of the substrate, the film growth can take place by ion-by-ion condensation of the material on the substrate or by adsorption of the colloidal particles from the solution on the substrate |40,42,43|. The process of precipitaton of a substance from the solution onto a substrate depends mainly on the formation of a nucleus and subsequent growth of the film. The concept of nucleation in solution is that the clusters of molecules formed undergo rapid decomposition and the decomposed particles combine to grow up to a certain thickness of the film beyond which no further building up of thickness occur. It is known that the nucleation starts at some local inhomogenity when ionic product exceeds the solubility product. Growth of these nuclei by the addition of more ions from the solution results in the formation of stable nuclei of the size greater than the critical size. Further, growth up to a particle size of 10 µm results in the formation of colloidal dispersion. These primary colloids as a result of adsorption starts nucleation forming thin, adherent and specularly reflecting films indicating the cluster by cluster growth of the film.

When ammonia is added in the reaction mixture, it helps to increase the adherence of Bi^{3+} and S^{2-} ions onto the substrates |44|. The stirring of the solution (churning of the solution with proper position of the substrates attached to the substrate holder) increases the rate of arrival of the ions on the substrates and hence speeds up the rate of coagulation of colloidal particles in solution. This results in precipitation of colloidal Bi_2S_3 particles which now cannot be adsorbed on the surface of the substrate leaving the chance for ion-by-ion growth of the films |40|. In our case we have experimented with both freshly prepared bismuth solution and bismuth solution kept for 4-5 hours prior to the Bi_2S_3 deposition. It is found that in the former case, good quality (very uniform, reproducible, tightly adherent, specularly reflecting) dark brown deposits are obtained while in the later, thick spotty, diffusely reflecting and relatively non uniform films are obtained.

2.4 Electronation and De-electronation Reactions .

The process by which the substance gains an electron is called electronation rection |45|:

$$OX + e^- \rightleftharpoons Red.\ E^0 \quad \text{--------------------} \quad 2.1$$

where, OX and Red are oxidised and reduced species respectively and E^0 is the standard electrochemical potential. The reverse of an electronation is de-electronation process, in which loss of an electron occurs. Thus the "REDOX" system is a combination of two species where, one species losses an electron, while other gains. The electron energy states in a redox electrolyte are analogous to the energy states in the solid by the energy change :

$$[\ OX\ Solv\ ] + e^{-}_{\infty} \rightleftharpoons [\ Red.Solv\ ] \text{ --------------- } \quad 2.2$$

in the reaction. This means that a free electron from infinity is introduced into the solution and it occupies the lowest energy state in an oxidised species (without change in solvation structure) called as energy of the unoccupied states. The process exactly reverse of this gives energy of the occupied states (reduced species). The summation of these occupied and non-occupied energy states gives the probability function as:

$$D_{redox}(E) = D_{red}(E) + D_{ox}(E) \qquad \ldots \quad 2.3$$

Which is similar to the density of states function in solids |46|.

The function $D_{red}(E)$ and $D_{ox}(E)$ can further be expressed as:

$$\left.\begin{array}{l} D_{red}(E) = C_{red}\,.W_{red}(E) \text{ and} \\ D_{ox}(E) = C_{ox}\,.W_{ox}(E) \end{array}\right| \qquad \ldots \quad 2.4$$

Where, W_{red} and W_{ox} are given by the thermal distributioon functions of ionic configurations and C_{red} and C_{ox} are concentrations of ions in solution.

Under equilibrium condition the occupation of these energy states in electrolyte is again given by the Fermidistribution functions as :

$$\left.\begin{array}{lll} D_{red}(E) & = D_{redox}(E) & [E - E_{F,redox}] \quad \text{and} \\ D_{ox}(E) & = D_{redox}(E) & [E_{F,redox} - E] \end{array}\right| \qquad \ldots 2.5$$

where, $E_{F,redox}$ is the chemical potential of electrons in redox electrolyte. A detailed mathematical analysis is made by Gerischer [46]. Both Metals and semiconductors can perform redox reactions with electrolyte [47]. The transfer of an electron to or from the solution can take place only in the energy region of the conduction band while that of the hole in the energy region of the valance band. Such transfer can occur between two states having same energy, one empty and other filled.

2.5 The Semiconductor/Electrolyte (S/E) Interface.

2.5.1 General.

The charge transfer across the semiconductor-electrolyte interface in dark or light results in the flow of current through the junction formed by the semiconductor and electrolyte. This is the key concept in the working of photoelectrochemical solar cells. The work of Brattain and Garrett [48,49], forms the basis of earlier studies of semiconductor electrolyte interfaces. Gerischer [50,53], deriving an analogy with semiconductor physics, has suggested that the oxidised and reduced species may be linked respectively with the conduction and valance bands (Non occupied and occupied energy states). A term $E_{F,redox}$ can also be defined similar to a semiconductor Fermilevel E_F. The energy necessary to transfer an electron from the reduced species to the oxidised species is analogous to tne band gap 'Eg', of a semiconductor and redox potential is a potential required to transfer an electron from a redox species to a vacuum level or vice versa.

The analogy between a semiconductor and an electrolyte is not perfect. The nature of charge carriers in the two phases is entirely different. One is electronic while other is ionic. In the semiconductors the environment seen by an electron is an "electron cloud" and its motion is under the periodic potentials of positively charged and fixed ion cores. In the electrolytes, ions move with an ionic cloud of opposite charge with or without change in solvation shell. As two phases are distinctly different, it would be interesting to know what happens when the two are brought in contact. Deep inside the semiconductor, the charge carriers are in an atmosphere of isotropic forces and that inside the electrolyte, net force on an ion is zero. Hence at the interface boundary picture is different. At the interface an ion is under the two different forces; one due to ions of an electrolyte and other due to the electrode.This anisotropy of forces at the boundary leads to a quite distinct structure of the interface compared to bulk structure. The anisotropic forces at the interfacial region results in a new arrangement of solvent dipoles and ions of the electrolyte and electrons of the electrode. This electrification of the electrode-electrolyte interface is shown in fig.2.1.

In the begining the anisotropy of forces at the interface makes the charge carriers to accumulate near the surface. When there is a sufficient build up of charges on both sides, the electrical forces at the surface overpower the barriers, resulting in the flow of charges. An equilibrium is established when the electrochemical potential on the electrode side (E_S) and on the electrolyte side (E_l) becomes equal);

i.e. $E_S = E_l$ ------------ (At equilibrium) ... 2.6

Thus the potential gradient associated with the interface region acts as a barrier for further flow of charges.

The potential gradient is high at the surface and gradually decreases as we move away from it, which gives rise to a double layer. A study of the double layer at the electrode-electrolyte interface is related to the charge transfer reactions, corrosion etc.

2.5.2 Structure of the double layer at the Electrode-Electrolyte Interface .

A qualitative picture in fig. 2.1 shows that the electrode-electrolyte interface gets rectified as a result

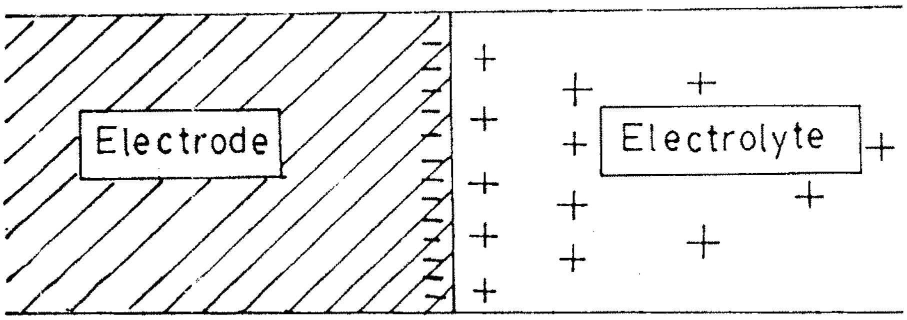

Fig.2.1 Qualitative description of charge distribution near the electrode/electrolyte interface.

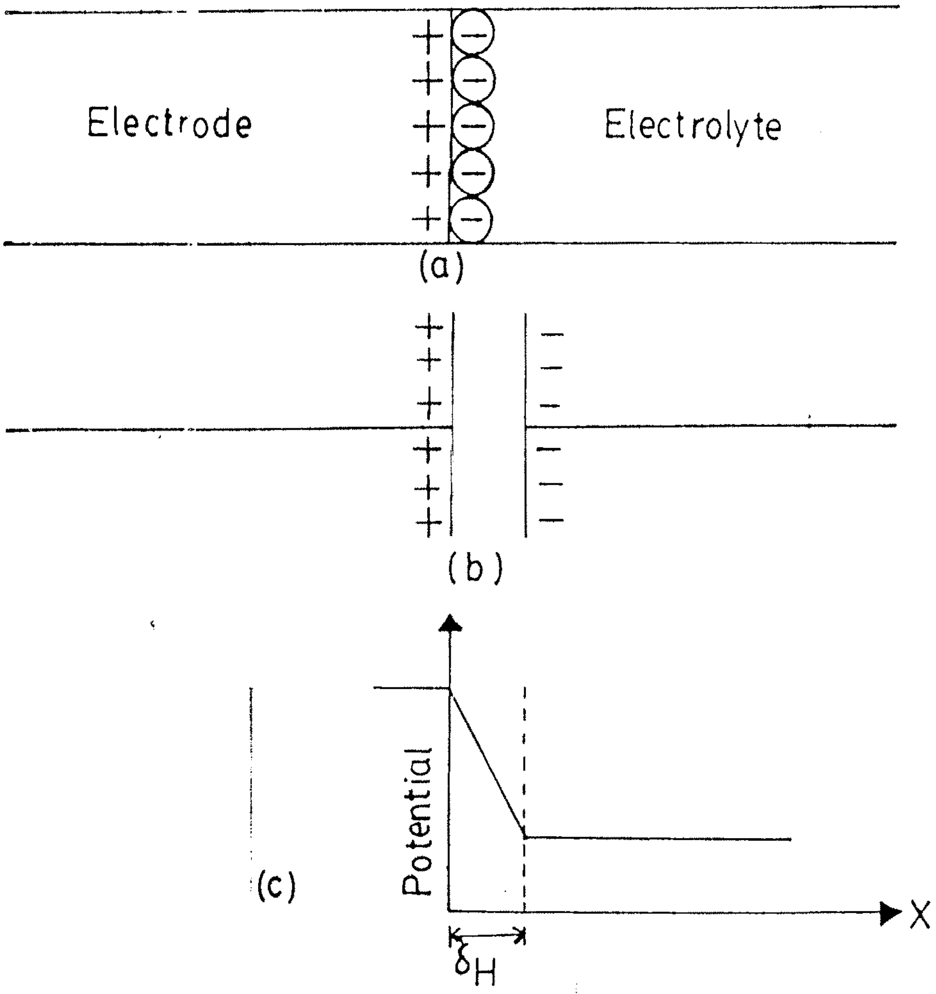

Fig.2.2 Helmholtz-Perin model :

a) Schematic charge distribution

b) Electrical equivalent of interface

c) Potential distribution towards the electrolyte.

BARR. BAL[illegible] KHARDEKAR LIBRARY
SHIVAJI UNIVERSITY, KOLHAPUR.

of a redistribution of charges. Upon emersion of a semiconductor into an electrolyte, the surface of the semiconductor acquires a net charge density. Both, semiconductor surface and electrolyte region near the boundary acquire potential distribution which decreases with distance from the phase boundary. The overall charge neutrality occurs when,

$$q_S = q_{el} \qquad \ldots 2.7$$

Where q_S and q_{el} are respectively charges near the semiconductor and electrolyte sides of the interface. To examine the structure of the double layer, we divide the interface into two regions :

a) Electrolyte side of interface, and

b) Electrode side of interface.

2.5.2.1 Electrolyte side of the interface.

Helmholtz |54| assumed that the charged layers of ions forms a sheath at the dipped metal surface as shown in fig 2.2 (a). The Helmholtz-Perrin model suggests the electrode-electrolyte interface as a parallel plates of condenser charged oppositely but with equal charges as shown in fig. 2.2 (b). The term double layer thus originated. All the potential is assumed to be dropped across the sheath of the ions of thickness 'δH' called to be a double layer separation. This 'δH' is initially assigned to be independent of the voltage applied to the electrode. If the charge on the capacitor is dQ and potential across the layer is dV, then the differential capacitor is given by,

$$C = \frac{dQ}{dV} = \frac{\epsilon \epsilon_0}{\delta_H} \qquad \ldots \; 2.8$$

where, $\delta_H = \epsilon_0 \epsilon \dfrac{dV}{dQ}$

where ϵ_0 and ϵ are the dielectric constants of the material and free space respectively. This voltage independency of δ_H or C is against the experimental observations. Gouy |55| and Chapman |56| suggested that the electrode surface on which charges have accumulated may be considered as a large central ion exerting a planar electrostatic field on the solution side of the interface. This force falls off slowly as one moves deeper into the solution bulk away from the electrode surface. Thus ions does not confine themselves to a plane as was suggested by the Helmholtz-Perrin model, but they form a diffuse layer as shown in fig. 2.3(a). This diffused ionic layer is called the "Gouy Layer". Fig.2.3(b) shows approximate potential distribution according to Gouy-Chapman theory and the charge distribution in the Gouy layer is given by the Poissons equation :

$$\Phi_{(x)} = \Phi_{(0)} \exp(-L_G \cdot x) \qquad \ldots \; 2.9$$

where, $\Phi_{(x)}$ = potential at any distance x in electrolyte,

$\Phi_{(0)}$ = potential at x = 0 and

L_G = Gouy Layer thickness or Debye length.

A
11683

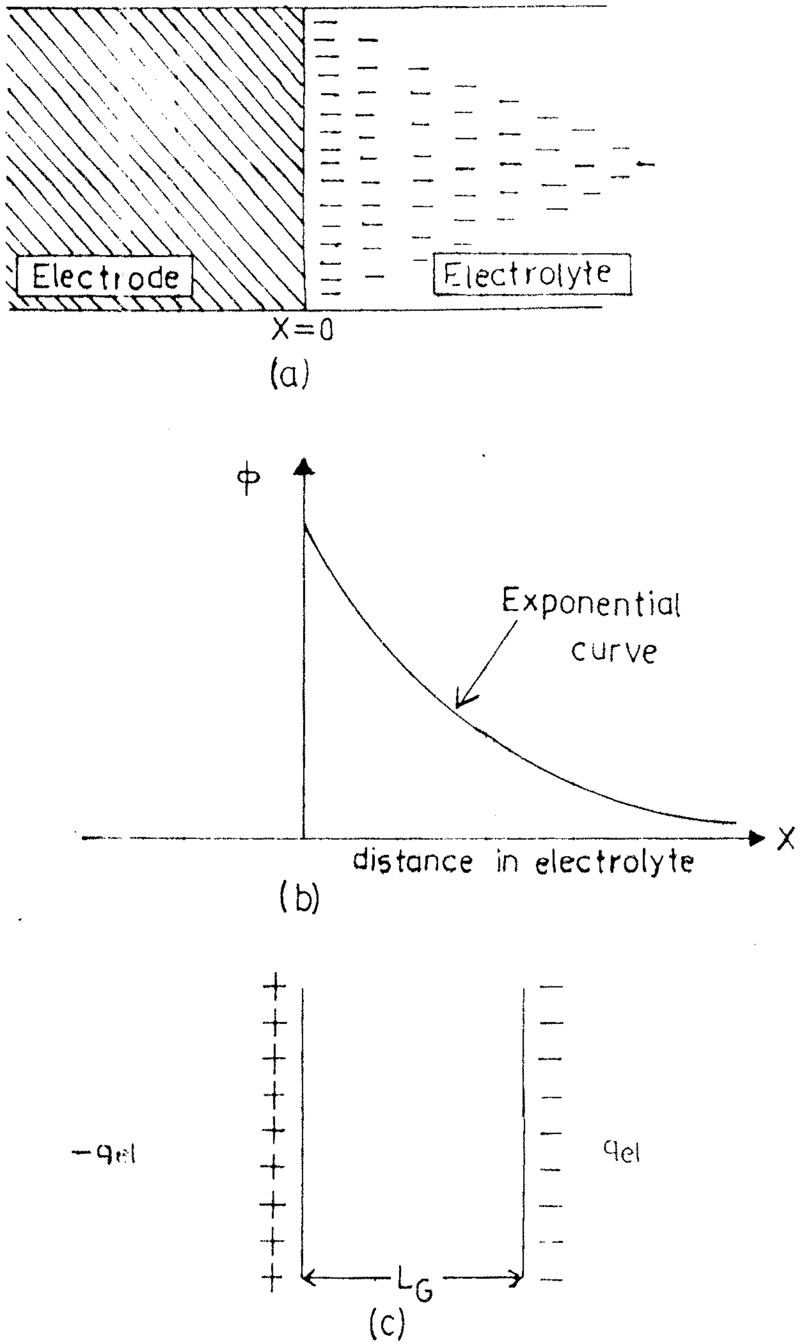

Fig.2.3.Gouy-Chapman model,(a) Schematic charge distribution
(b) Potential distribution in the electrolyte,
(c) Simulated electrical equivalent.

It was found that : i) Charge density distribution in Gouy Layer decays exponentially with distance in the electrolyte. ii) Thickness, L_G varies inversely with square root of the ionic concentration and iii) Differential capacity of the Gouy layer is voltage and concentration depenedent.

Stern |57| predicted that the ions, being of finite size, keep a minimum distance of approach to the electrode surface. Thus double layer is neither abrupt nor diffused but a combination of the two. The situation is shown in fig.2.4. Here interface distribution is divided into two layers

i) Dense : Here ions stuck to the electrode and potential variation is linear.

ii) Diffused : Formed as a result of opposing tendencies of the attractive coulombic force and disordering thermal fluctuations where potential decays exponentially as shown in fig. 2.4. (b).

The stern model does not explain explicitly how the ions are stuck to the electrode. The probable reason may be the hydrated electrode surface and stripping off solution. The stripping off solution means pushing some water molecules away and sit inclose contact with the electrode by stripping off their solvation. The ions so sitting are called "contact adsorbed ions". The locus of all such contact adsorbed ions form the "Inner Helmholtz Plane (IHP)". The solvated ions are

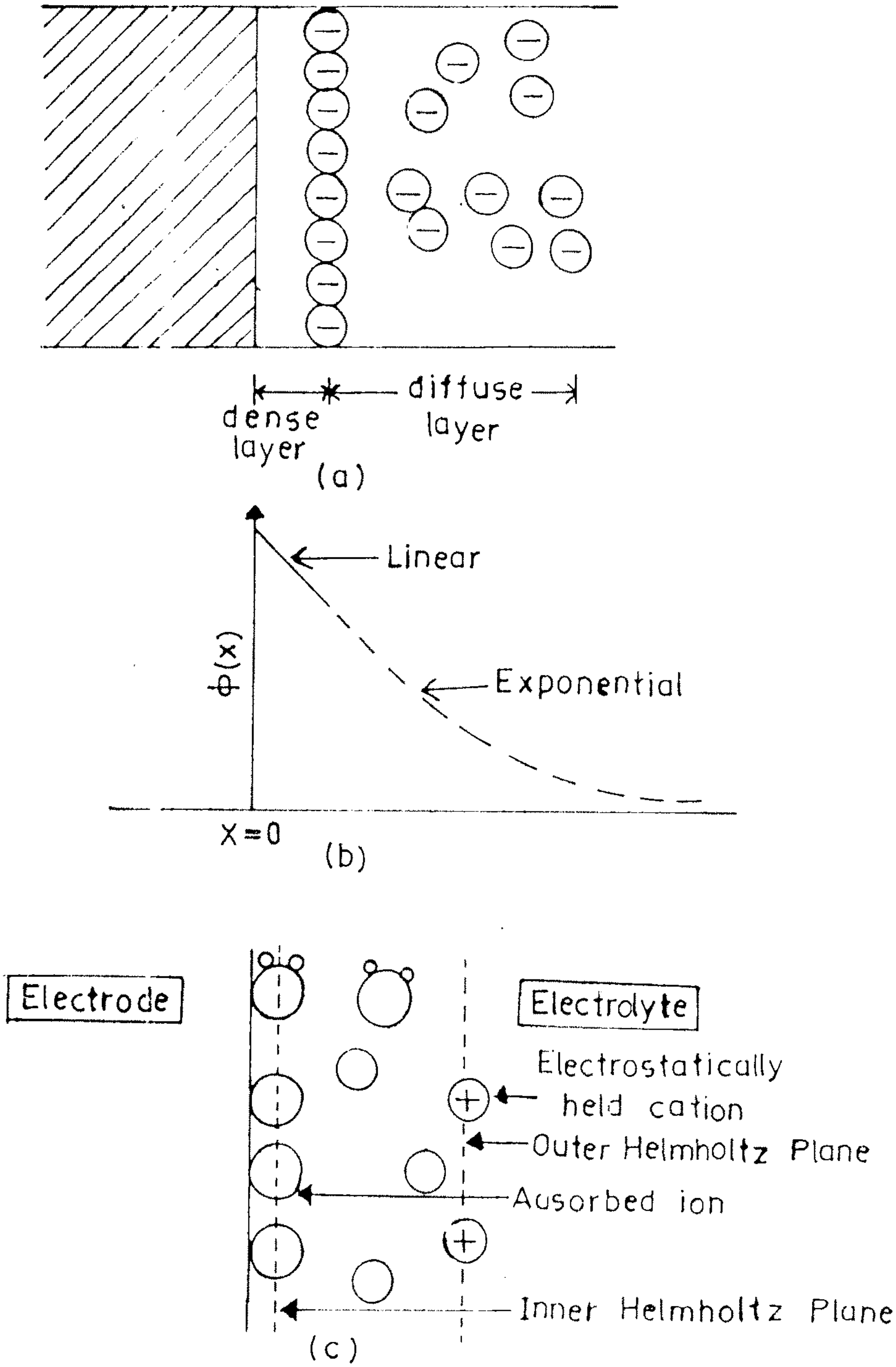

Fig.2.4.Stern model, (a) Schematic charge distribution,
(b) Potential distribution,
(c) Relative positions of inner and outer Helmholtz planes of electrode/electrolyte interface.

SHIVAJI UNIVERSITY LIBRARY KOLHAPUR

in the "Outer Helmholtz Plane (OHP)".The situation is shown in fig. 2.4 (C).

Thus a picture of electrolyte side of the interface can be summarised as;

i) The IHP consisting of water dipoles and specifically adsorbed ions which forms a saturated dielectric layer with a dielectric constant equal to 6.

ii) The OHP consisting of solvated ions at a distance of their closest approach to the elctrode surface. The degree of orientation decreases with distance from the electrode surface, hence OHP consist of partially oriented water molecules with dielectric constant between 6 and 78. A mean value of about 40 is usually taken.

iii) Gouy layer due to disordering of thermal fluctuations and the ordering electrical forces tend to form diffuse ionic layer. Thus G-C theory fails near the electrode surface. Thus Stern's suggestion has to be considered. For all practical purposes, G - C - S theory is correct at low ion concentration. At high ionic concentration, the screening charge clouds assumes a layered structure |58|. Recently, Liu has developed a Lattice-Gas model based on above ideas where both ions and solvent molecules are taken as hard spheres of equal radii and they are assumed to form a parallel layers near the planar electrode as shown in fig. 2.5. The lattice parameter is chosen as the distance of closest aproach of two

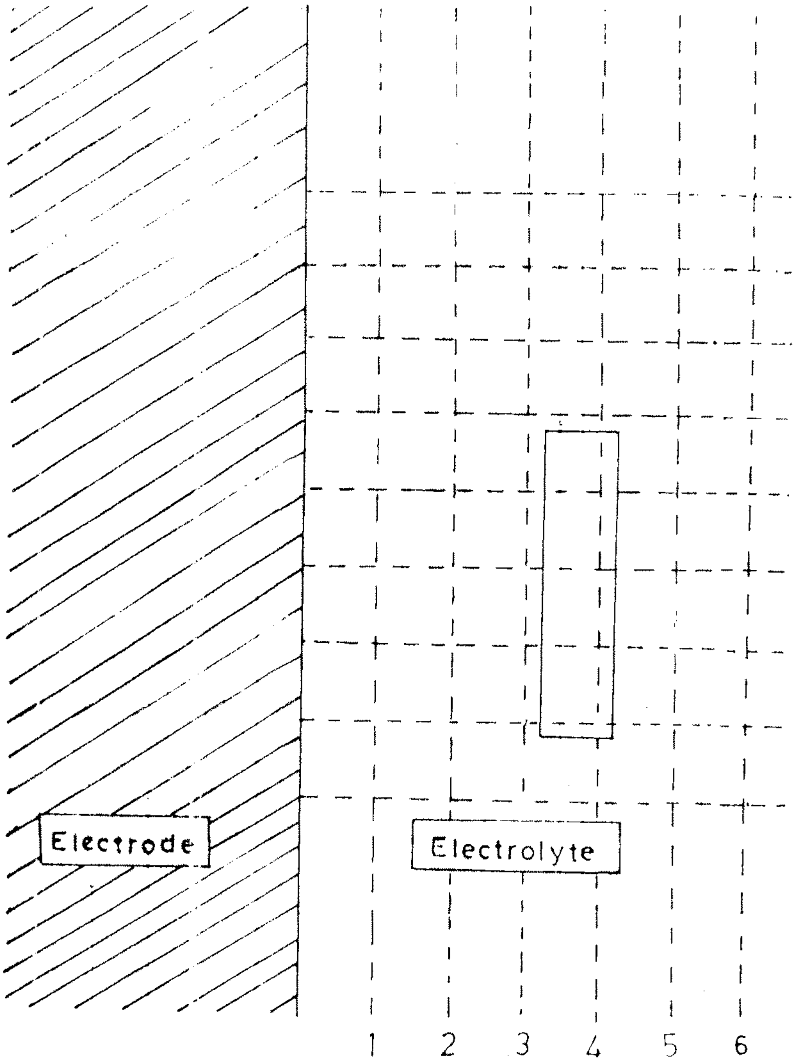

Fig.2.5 Hypothetical lattice model of the metal/electrolyte interface (Liu's model).

molecules. Liu's model gave reasonable description of the properties of the electrolyte in the interface region and was better than the all earlier models. For detailed discussion reader may refer to Bockris and Reddy |59|, Parsons |60|, Delaphy |61| and Barlow |62|.

2.5.2.2 Semiconductor side of the interface.

The first systematic investigation of the semiconductor surface in contact with an electrolyte was reported by Brittain and Garret|48| . Many references are now available with excellent aspects of semiconductor electrochemistry |52,53,59,63 -67|.

It may be recalled that the anisotropic forces at the electrode-electrolyte interface and a charge transfer across the interface leads to the rearrangement of electrons and ions. The charge distribution of the electrode side are widely different for metals and semiconductors principally because :

i) Electrons and holes are charge carriers in semiconductors while in metals only electrons carries the charges.

ii) The charge carrier density in the semiconductor is now (10^{19} to 10^{23} cm^{-3}) as against in metals (10^{28} cm^{-3}).

iii) For metals the charges are located at the surface while for semiconductors they forms a space charge layer within the semiconductor near the interface.

The potential and charge distribution on the electrode side of the semiconductor-electrolyte and metal-electrolyte interfaces are given in fig.2.6 (a,b). The nature of the space charge layer depends upon the manner in which charge transfer occurs across the interface.

Three types of situations can arise :

i) If semiconductor acquires excess majority carriers the space charge layer is termed an "enrichment layer" such a layer leads downward band bending for n-type while upward for p-type semiconductors.

ii) If surface becomes depleted of majority carriers then space charge is known as "depletion layer" . This leads to upward band bending for p-type semiconductors.

iii) If charge distribution is such that the minority carrier concentration at the surface is greater than that within the bulk. Space charge layer under this condition is called as "inversion layer". This leads to a large upward bending for n-type and downward for p-type. The above three situations are shown in fig. 2.6 (c,d).

According to Braittain and Garrett the charge distribution and potential in the space charge layer can be formulated by solving poisson's equation and can be linearised to first approximation. Subsequently, the potential drop in the space charge layer can be expressed as

$$\Phi = \Phi_0 \exp. (-L_G X) \qquad \ldots 2.10$$

where

$$L_D = \frac{(\epsilon_s \epsilon_o K \cdot T)^{1/2}}{2 n_i q^2}$$

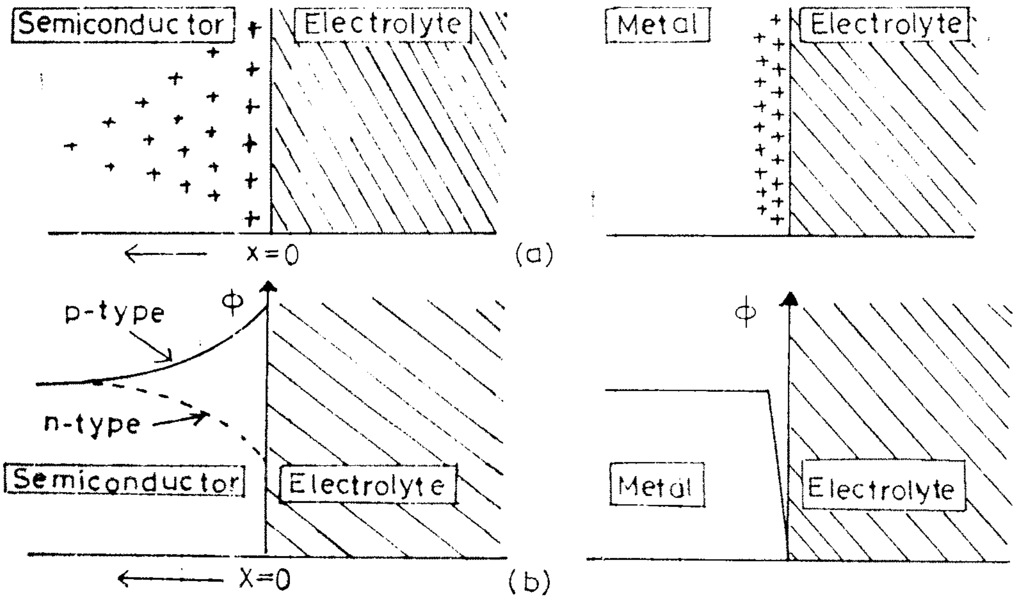

Fig.2.6 Difference between metal/electrolyte and semiconductor/electrolyte interface :
a) Charge distribution b) Potential distribution

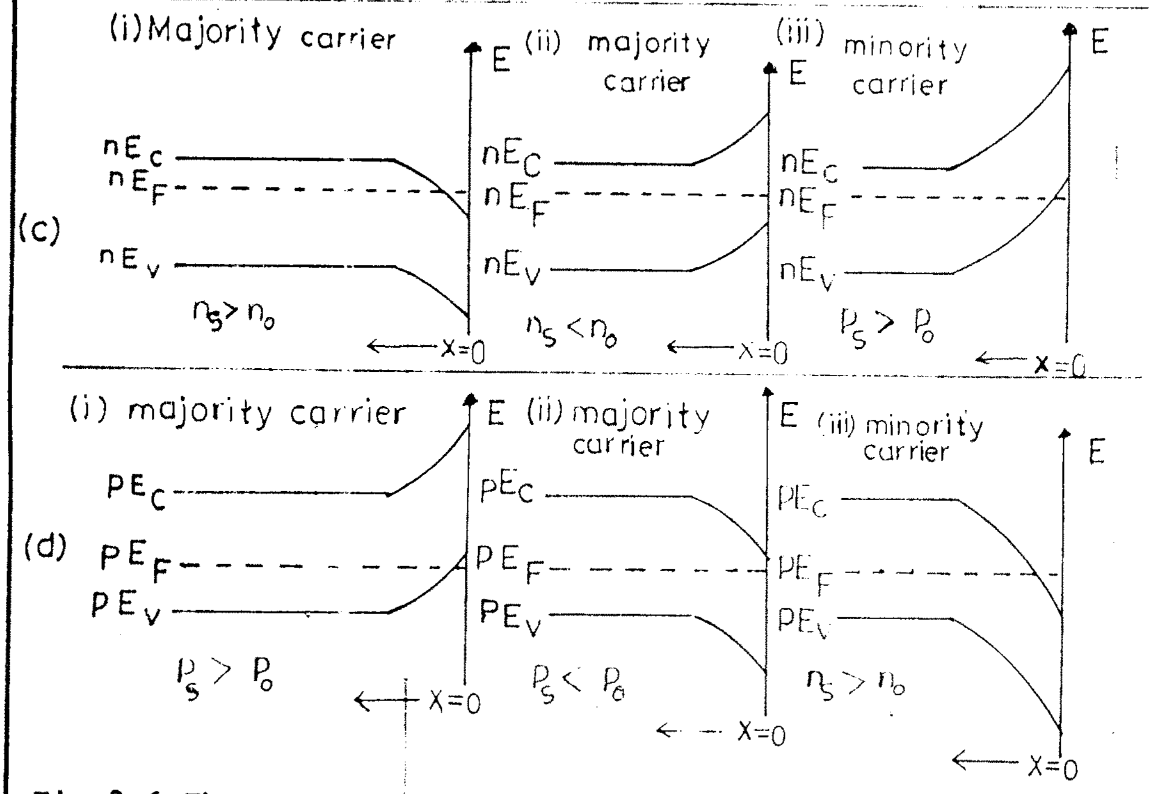

Fig.2.6 Three types of space charge layers namely enrichment, depletion and inversion at :

c) n - type semiconductor

d) p - type semiconductor

L_D' is called as Debye length and gives the extent of space charge layer. The potential drop in the space charge layer is, therefore, exponential. For n-type semiconductors,

$$L_D = \left[\frac{(\epsilon\epsilon_0 k \cdot T)}{2 N_D q^2}\right]^{1/2} \qquad \ldots\ 2.11$$

The profile of potential distribution according to equation (2.10) is shown in fig. 2.6 (b). Equation (2.11) clearly shows that , L_D varies as the inverse square root of the carrier concentration.

i.e. $L_D \propto 1/\sqrt{N_D}$

When N_D is very high, L_D becomes very small and all the charges on electrode side then confine near the surface; a case similar to the metal electrodes.

2.5.2.3 Role of surface states and surface adsorbed ions.

The potential and charge distribution at the electrode-electrolyte interface are affected by the surface states and surface adsorbed ions at the interface. Surface states are essentially the results of non-periodicity of the lattice at the boundary which lead to the formation of electronic states localised at the surface. They can further be formed by the adsorption of foreign atoms or ions. The surface states act as a traps for charge carriers and hence substantially modify the space charge, Gouy and Helmholtz layers. Adsorption at the surface can also substantially change the charge and potential distribution in the various

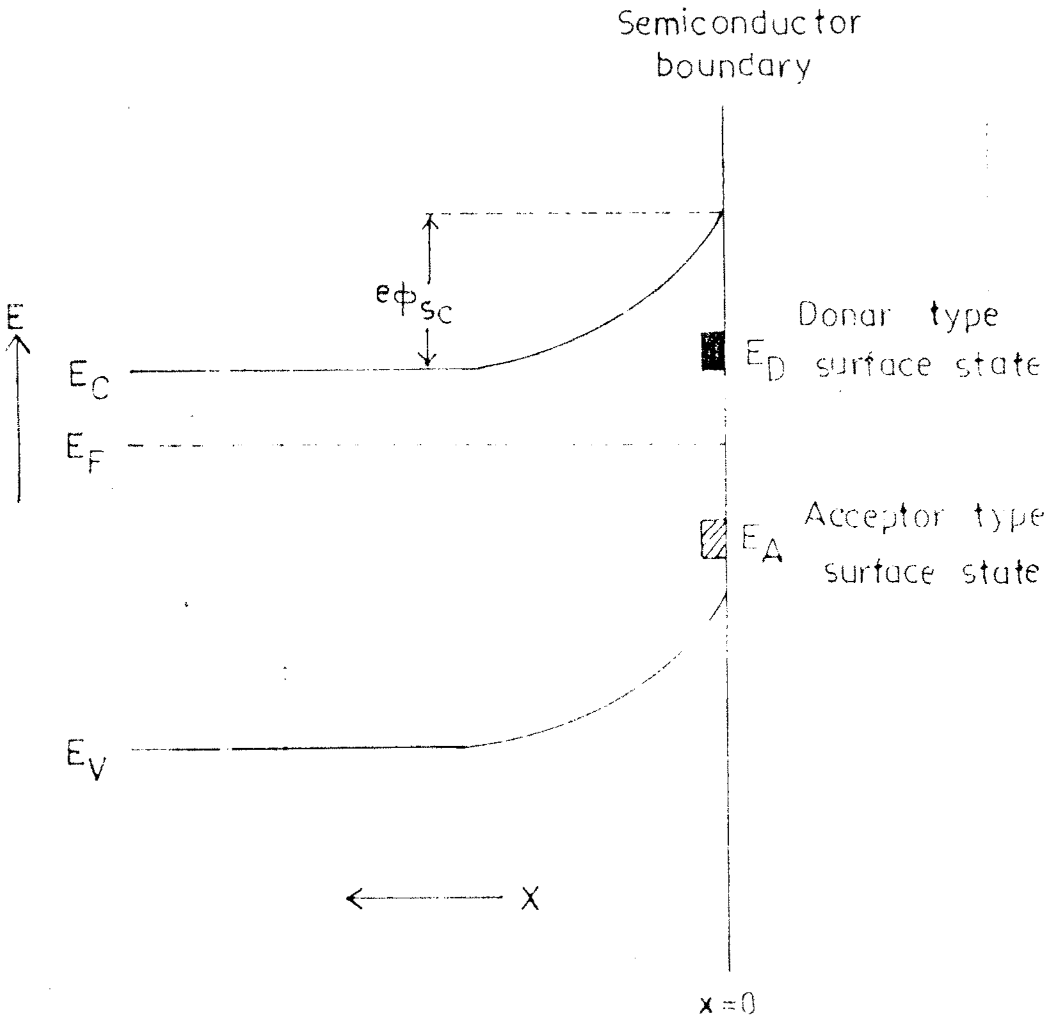

Fig.2.7 Energy level diagram showing schematically the position of surface states with energy E_A and E_D.

regions of the electrode-electrolyte interface.

2.5.2.4 Complete picture of the electrode-electrolyte interface.

The resulting picture of the semiconductor electrolyte interface consists of the following :

i) Diffused space charge layer in the semiconductor (including surface states and adsorbed ions),

ii) Helmholtz layer,

iii) Gouy layer.

The charge distribution at the semiconductor electrolyte interface appears somethwat qualitatively symmetrical. The total charge on the semiconductor side of the interface is,

$$q_s = q_{sc} + q_{ss} + q_{ads} \qquad \ldots\ 2.12$$

The electroneutrality demands :

$$q_s = q_{sc} + q_{ss} + q_{ads} = q_{el} \qquad \ldots\ 2.13$$

where q_{sc}, q_{ss}, q_{el}, q_{ads} corresponds respectively to charges in the space charge, surface states, electrolyte and due to adsorbed ionic groups. The actual distribution of charge carriers may be quite complicated and it is doubtful whether M.B. or F.D. statistics are applicable to the theory of space charge layer under strong field at the boundary and 'L_D' is comparable with length of an electron wave in semiconductor. The potential distribution is given in fig.2.8 (c).The total

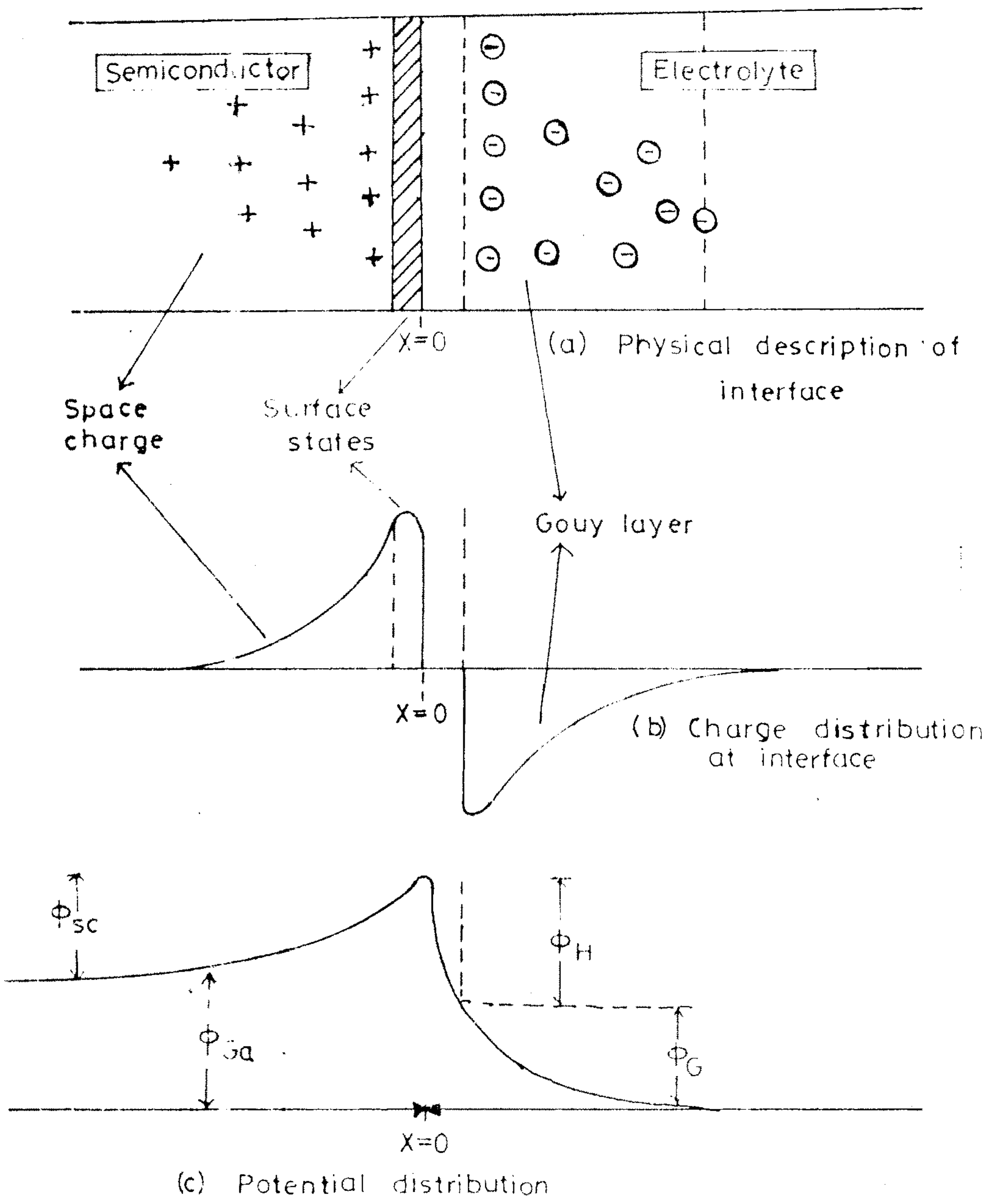

Fig.2.8 Charge and potential distribution at the S/E interface. ϕ_{sc}, ϕ_H, ϕ_G and ϕ_{Ga} are respectively potentials across the space charge, Helmholtz layer, Gouy layer and galvanic potentials.

(a) Physical description of interface,
(b) Charge distribution at interfacem
(c) Potential distrobution.

potential Φ_{Ga} is :

$$\Phi_{Ga} = \Phi_{SC} + \Phi_{G} + \Phi_{H} + \Phi_{SS} \quad . \qquad \ldots\ 2.14$$

For concentrated electrolyte solutions potential drop across the Helmholtz and gouy layers can be neglected compared with space charge layer which is generally the case for PEC solar cells.

2.5.3 Electrical equivalent of double-layer and differential capacitance :

Neglecting surface states and adsorption as a first approximation, the simplest electrical equivalent of a S-E interface can be regarded as a series combination of three capacitances ; C_{SC}, C_H and C_G . The total capacitance is given by

$$\frac{1}{C_T} = \frac{1}{C_{SC}} + \frac{1}{C_H} + \frac{1}{C_G} \qquad \ldots\ 2.15$$

For moderately concentrated electrolyte, the contribution to C_T by C_H and C_G can be ignored. Thus the total capacitance is solely that due to a space charge layer. As is well known that surface states deteriorate the performance of PEC cell, a model to account for the behaviour of surface states can be incorporated into an equivalent circuit of the interface as shown in fig.2.9 |53,67|.

Each of n-surface states is represented as a series combination of a capacitance (C) and a resistor (R). The surface states are in parallel with each other and the

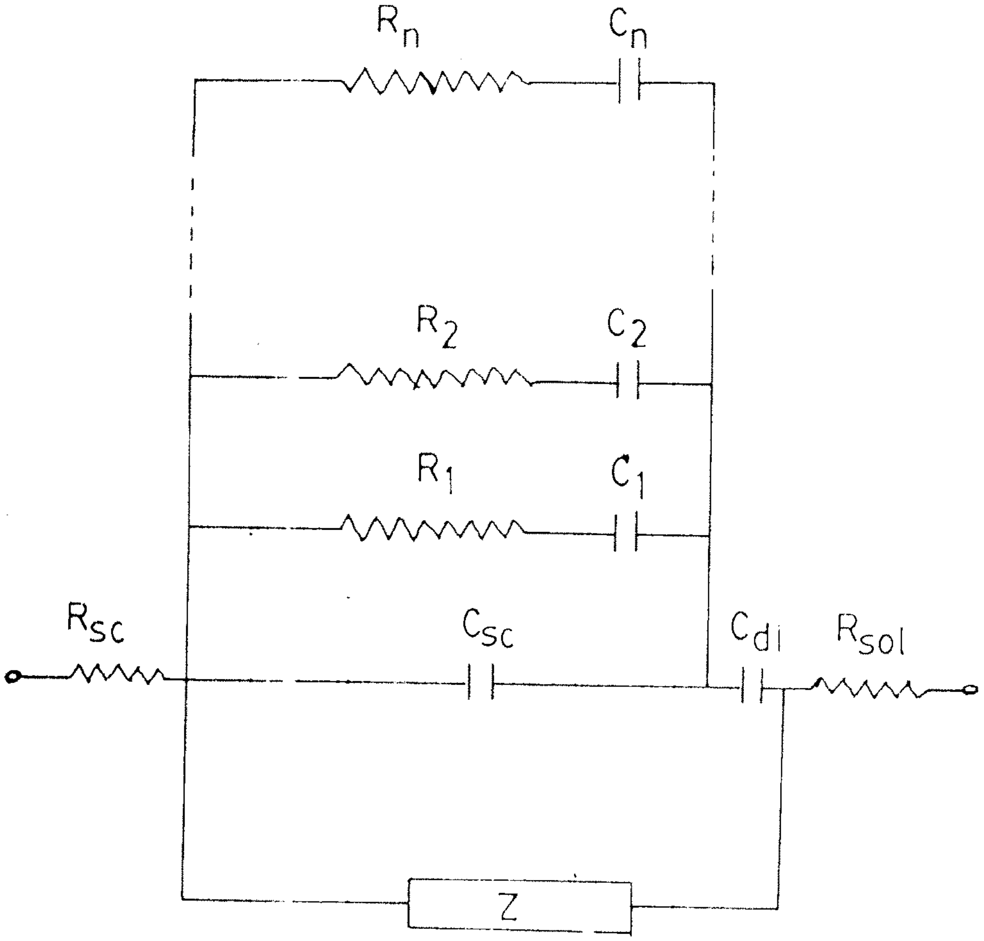

Fig. 2.9 An equivalent circuit for the semiconductor/ electrclyte interface.

semiconductor space charge capacitance (C_{sc}). The total electrode capacitance, therefore, is $C_{sc} + \sum Ci$. This network of parallel capacitors is in series with the bulk resistance (R_{sc}) of the material, the double layer capacitance (C_{dl}), and the solution resistance (R_{sol}) between the semiconductor and the reference electrode. Because the potentiostat maintains potential control between the reference electrode probe and the contact on back of semiconductor, the remainder of the solution and counter electrode impedances have no effect under usual conditions and therefore are not included in the equivalent circuit. Any Faradaic process will short across C_{sc} and C_{dl} as represented by Z. The analysis was simplified by controlling the conditions to minimise any Faradaic process so that Z can be replaced by an infinite impedance. Also C_{dl} is much larger than C_{sc} and can be ignored |53,67|.

2.5.4 Space charge capacitance and the Mott-Schottky plot.

The electrode electrolyte interface can further be analysed to obtain the flat band potential. Thus the measurement of differential space charge layer capacitance provides a convenient tool, for obtaining the useful informations about both the semiconductor and an electrolyte. As discussed earlier for semiconductor electrolyte solar cells, the contribution to the capacitance is through capacitances due to depletion region, Helmholtz layers and the Gouy diffused layer. Neglecting the surface states and assuming all the donors and acceptors as fully ionised and high ionic concentration of the redox couple the space charge layer capacitance is given by :

$$C_{sc} = \frac{\epsilon_s \epsilon_0}{L_D} \frac{\left[-\lambda \exp(-Y) + \lambda^{-1} \exp(Y) + (\lambda - \lambda^{-1})\right]}{\left[\lambda\{\exp(-Y) - 1\} + \lambda^{-1}\{\exp \cdot Y - 1\} + (\lambda - \lambda^{-1})Y\right]^{1/2}} \qquad \ldots\ 2.16$$

where,

$$\lambda = \left[\frac{P_0}{n_0}\right]^{1/2} \text{ and } \quad Y = q\left[\frac{\phi(x) - \phi(0)}{KT}\right] \qquad \ldots\ 2.17$$

where $\Phi(x)$ = potential at a distance x in the space charge layer ,

$\Phi(0)$ = potential at the boundary i.e. at x=o,

ϵ_s = dielectric constant of the semiconductor,

ϵ_0 = permittivity of the free space,

and other terms have their usual significance. For intrinsic semiconductors,

$n_0 = p_0 = n_i$ and $[p_0 / n_0]^{1/2} = 1$

Hence equation (2.16) reduces to :

$$C = \frac{\epsilon_0 \epsilon_s}{L_D} \cosh \frac{(q\, \Phi_{sc})}{KT} \qquad \ldots\ 2.18$$

The capacitance vs. voltage curve is symmetrical as shown in the fig. 2.10.

The space charge capacitance passes through a minimum at Φ_{sc} = 0, a situation corresponding to a flat band potential. Equation (2.18) is valid for small band bending

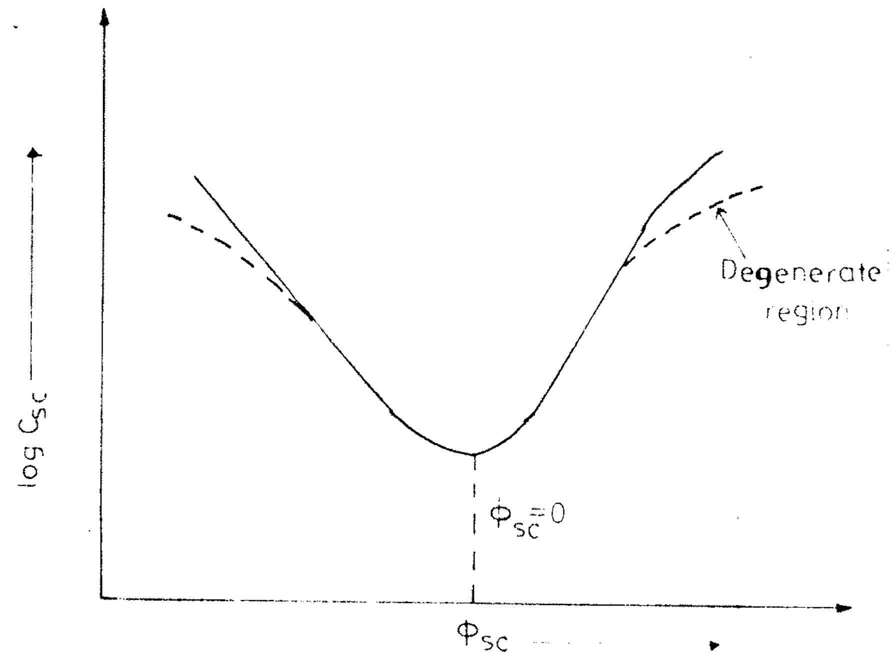

Fig.2.10 Schematic C_{sc} vs. ϕ_{sc} plot for intrinsic semiconductor.

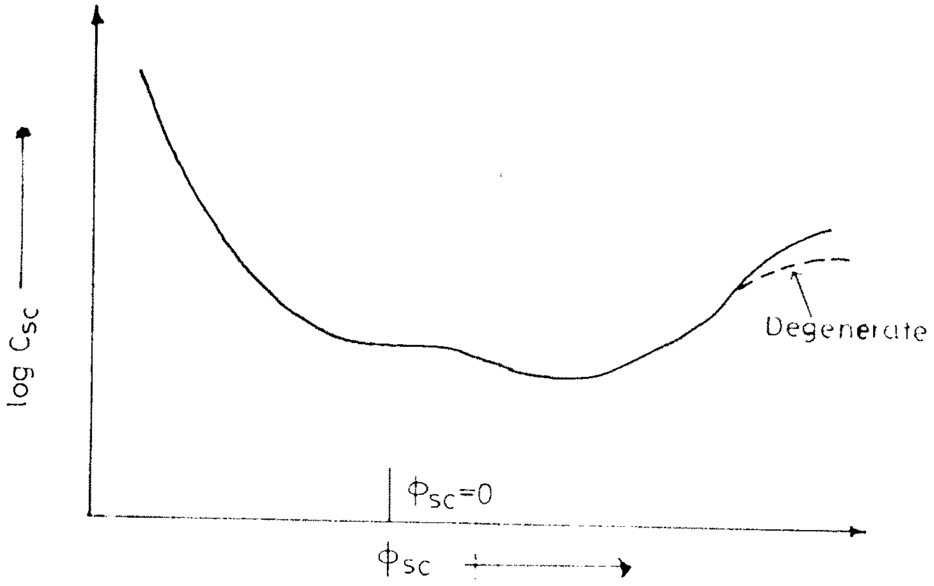

Fig.2.11 Schematic C_{sc} vs. ϕ_{sc} plot for doped n-type semiconductor.

and is limited by the bandgap. When $\Phi_{sc} = Eg/2$, further accumulation of charges become restricted by the density of states and degeneracy begins. This slows down further increases in capacity as shown in fig. 2.10

For heavily doped n-type semiconductor, $n_0 >> p_0$ & $\lambda^{-1} >> \lambda$.
For negative electrostatic potential in space charge,
$|Y| >> 1$ and $\lambda e^{-Y} << \lambda^{-1}$ and equation 2.16 simplifies to :

$$C_{sc} = \left[\frac{\epsilon_0 \epsilon q N_D}{2}\right]^2 \left[\Phi_{sc} - \frac{kT}{q}\right] \quad \ldots \quad 2.19$$

The C_{sc} vs. Φ_{sc} plot for this case is depicted in fig. 2.11. The curve is similar, though somewhat flattened. Equation 2.19 can be rewritten and a more informative equation is obtained as :

$$\frac{1}{C_{sc}^2} = \frac{2}{\epsilon_0 \epsilon_s q N_D}\left[\Phi_{sc} - \frac{kT}{q}\right] \quad \ldots \quad 2.20$$

Equation (2.20) is called as the Mott-Schottky equation, according to which $1/C_{sc}^2$ vs. Φ_{sc} plot is a straight line. However , Φ_{sc} cannot be measured directly. Generally electrode potentials are measured against a reference electrode (NHE or SCE). The measured potential difference V corresponds to:

$$V = \Phi_{sc} - \Phi_{NHE} \quad \ldots \quad 2.21$$

The importance of Mott-Schottky plot is to find the flat band potential (V_{fb}). For $\Phi_{sc} = 0$, the bands are almost flat, and the Mott-Schottky equation can be written as:

$$\frac{1}{C_{sc}^{2}} = \frac{2}{\epsilon_s \epsilon_c q N_D} (V - V_{fb} - KT/q) \qquad \ldots \quad 2.22$$

Therefore, a plot of $1/C_{sc}^{2}$ vs.electrode potential 'V' will be a straight line and intercept with the voltage axis gives the value of 'V_{fb}'and the slope gives the donor concentration. The diagrammatic representation is shown for n and p type semiconductors in fig. 2.12.Further, the Mott-Schottky plot determines the type of majority carriers and the band bending,'V_b 'which is a maximum open circuit voltage obtained from a PEC cell. The 'V_b ' is related to 'V_{fb}' as :

$$V_b = \left[\frac{E_{F,redox}}{q} - V\right] \qquad \ldots \quad 2.23$$

where, $E_{F,redox} = -(4.5qV_{NHE} + qV_{redox})$ ... 2.24

Thus values of V_{redox} for many redox couples can be obtained from the data given by Latimer |68| and Lewis et al |69|.

The depletion layer width and position of the band edges can be calculated using Mott-Schottky plots. The majority carrier depletion layer width 'W' can be calculated from the following relation :

$$W = \left\{\frac{2\epsilon_o \epsilon_s}{q \cdot N_D} \left[V - V_{fb} - \frac{KT}{q}\right]\right\}^{1/2} \qquad \ldots \quad 2.25$$

and the position of band edges can be calculated from the electron and hole density in conduction and valance bands as:

specific adsorption of ions. From equation (2.30) when $\Delta\phi_H = 0$, E_A, V_S, V_{fb} yield a straight line plot otherwise there wolud be considerable deviation from the straight line behaviour.

In the derivation of the equation (2.22) the effects due to the electrolyte or semiconductor bulk resistance, interface as a leaky capacitor (Faradic currents) and frequency dependent dielectric constant were not taken into account and hence Mott-Schottky plots under such circumstances become frequency dependent as shown below in fig. 2.13 (a,b).

The plots show different intercepts (fig.a) and convergence (fig.b) along voltage axis for different frequencies. Case (a) occurs because of ion or dipole relaxation or adsorbed water dipole layer on the surface of a film which introduces an extra capacitance in series with frequency independent capacitance of the space charge layer. The case (b) occurs because of the deviation from the perfect periodicity of the lattice near the surface or due to mechanical damage of the surface|72|. The presence of surface states gives very complicated structure of the Mott-Schottky plots. Surface states can exchange the carriers with either to the band or to both by electrostatic coupling characterised by a time constant. This leads to the frequency dispersion in Mott-Schottky plots|65|. Since the capacitor C_{SS} changes with both the applied voltage and signal

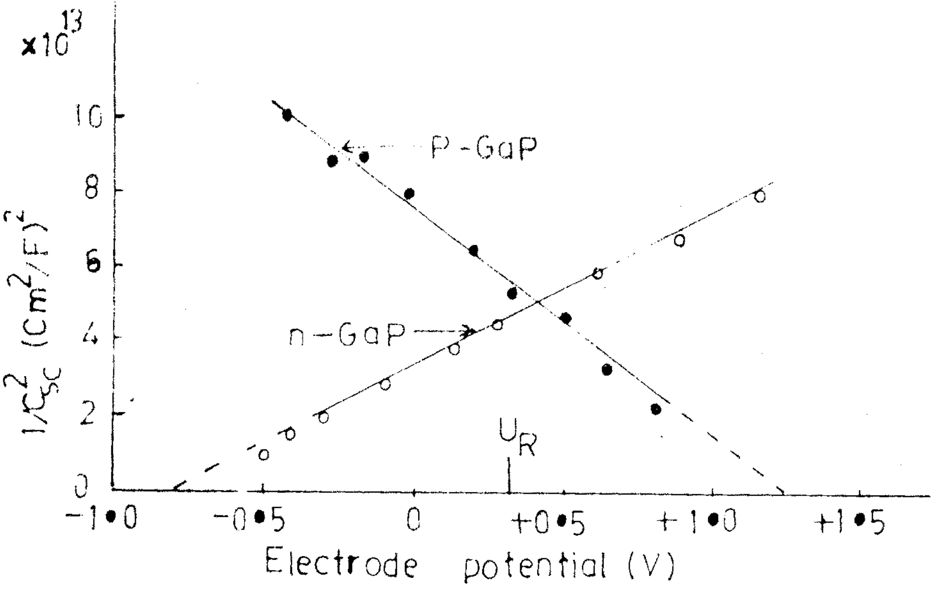

Fig.2.12 Mott-Schottky plots of space charge capacity for Gap electrodes vs. electrode potential in 1M-H_2SO_4.

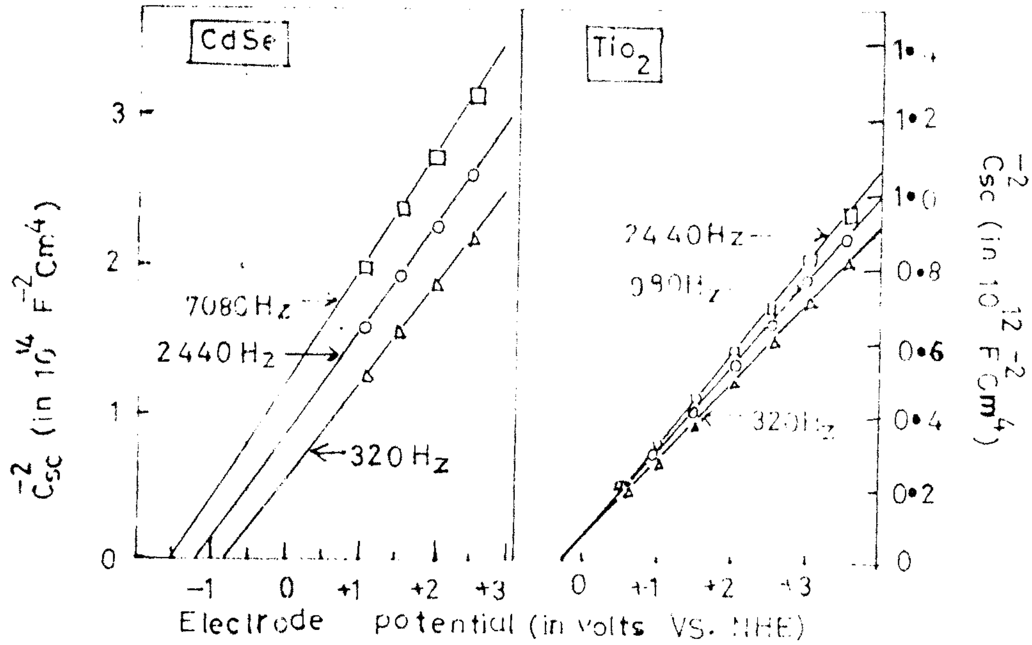

Fig.2.13 Mott-Schottky plots for : (a) CdSe (b) TiO_2 at different frequencies

(electrode potential in Volts vs. NHE).

$$\left.\begin{aligned} n_o &= N_c \exp(E_c - E_F/KT) \\ \text{and} \quad p_o &= N_V \exp(E_F - E_V/KT) \end{aligned}\right| \qquad \ldots\ 2.26$$

where, N_c and N_V are density of states respectively for conduction and valance bands; E_c and E_V are respectively conduction and valance band edges.

Equation (2.26) gives ;

$$\left.\begin{aligned} E_c &= E_F - KT.\ln\left(\frac{n_o}{N_c}\right) \\ \text{and} \quad E_V &= E_F + KT.\ln\left(\frac{p_o}{N_V}\right) \end{aligned}\right| \qquad \ldots\ 2.27$$

Under equilibrium $E_F = E_{F,redox}$ and using equation (2.24) E_c and E_V can be obtained.

The ideal Mott-Schottky behaviour is more an exception than a rule for the semiconductor-electrolyte interface. The departure from an ideal behaviour has been observed for many semiconductors by various workers| 70-74|.Some of the reasons for this non ideality are i) Geometrical factors such as the edge effect , non-planar interface, surfface roughness etc. leading to non-uniform a.c. current distribution , ii) Non-uniform doping iii) Presence of both donor and acceptor impurities iv) Presence of deep donors and acceptors, and v) An extra contribution, 'C'' to the total capacitance due to ;

a) the presence of an oxide film,

b) ionic adsorption on the surface,

c) Helmholtz layer capacitance,

d) existence of an acid-base equilibrium at the interface.

The total capacitance is now,

$$\frac{1}{C^2} = \frac{1}{C'^2} + \frac{2}{\epsilon_o \epsilon_s q N_D}\left[V - V_{Fb} - \frac{KT}{q}\right], \qquad \ldots \; 2.28$$

Under such condition $1/C^2$ vs.V plot would give N_D but not V_{fb} unambiguously unless 'C'' is known. To illustrate the above point an interesting example of the pH dependence of 'V_{fb}' observed for oxide semiconductor in contact with electrolyte is as |75|:

$$M - O + H_2O \rightleftharpoons M^+ - OH + OH^- \quad \text{and}$$

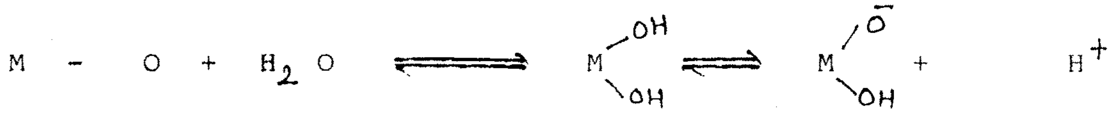

$$M - O + H_2O \rightleftharpoons M(OH)_2 \rightleftharpoons M(O^-)(OH) + H^+$$

The above equilibrium conditions indicate charge separation. One part is attached to the electrode and other is in solution. Thus potential drop across Helmholtz layer would vary with pH. The variation is described by the following relation :

$$\delta\Phi_H = \text{constant} + 0.059 \text{ pH} \qquad \ldots \; 2.29$$

Thus Mott-Schottky plot would be a set of parallal lines for different pH values.Butler and Ginley |76,77| correlated the pH dependance of V_{fb} to electron affinity (E_A) as :

$$E_A = E_o + V_{fb} + \Delta_{fc} + \Delta\Phi_H \qquad \ldots \; 2.30$$

where ,' E_o' is constant relating to the reference electrode and vacuum level (E_o = -4.75 for SCE and E = -4.5 for NHE), Δ_{fc} = correction factor approximately equivalent to doped fermi level and bottom of the conduction band.

$\Delta\phi_H$= potential drop across Helmholtz layer due to frequency, reliable data on V_{fb} and N_D can be obtained only when the experiments are performed on well etched samples. Mott-Schottky relation completely fails to determine 'V_{fb}' and N_D when sample thickness is less than the space charge layer |78|.

2.6 Charge-Transfer Mechanism Across The Semiconductor/ Electrolyte Interface.

In the foregoing (section 2.5) discussion we have seen how the charge exchange between a semiconductor and an electrolyte affects the potential and charge distribution inside the semiconductor and electrolyte without going into the details of actual charge transfer reactions. Excellent reviews on charge transfer reactions are now available by many authors |2, 64,65, 79-81|. The ions in the electrolyte are constantly under thermal motion. They keep striking the semiconductor electrode. Under suitable values for valence band, conduction band and redox energies , an electron may either be transferred from the electrolyte to electrode and vice-versa. Depending on the sign, the ionic species will either be reduced or become oxidised. In an idealised charge transfer reaction,semiconductor acts only as donor or acceptor for electrons without any chemical changes in its constitution.

2.6.1 Charge transfer in dark :

If the positive ions can move from the solution side to the electrode, they can jump back in the reverse direction. There occurs both electronation,

$$A^{+} + e^{-} \dashrightarrow D$$

and de-electronation

$$D \dashrightarrow A^{+} + e^{-}$$ reactions |59|. If a positive ion moves against the filed direction in an electronation reaction it moves in the direction of field in de-electronation reaction. This is shown in fig. 2.14 (a). Further, if the positive ions has to be activated through a potential difference '$\beta\Delta\bar{\phi}$' in electronation reaction, it has to be activated through the remainder ($1 - \beta\Delta\bar{\phi}$) in the de-electronation reaction; where β is symmertry factor and $\Delta\bar{\phi}$ is potential through which ion passes. Hence the electrical work for activation of reverse reaction is $+ F[(1-\beta) \Delta\phi]$, the plus sign is because of the direction of ion transfer and field are the same. Therefore the rate of de-electronation reaction becomes,

$$\overleftarrow{\nu}_e = \overleftarrow{K}_c\, C_D \exp.(1-\beta).F\,\Delta\bar{\phi}/RT \qquad \ldots\ 2.31$$

and de-electronation current density is

$$\overleftarrow{i} = F.\overleftarrow{K}_c\, C_D \exp(1-\beta)F\frac{\Delta\phi}{RT} \qquad \ldots\ 2.32$$

There must be some value of $\Delta\bar{\phi}$ at which the rate of loss of electrons and gain of electrons by the electrode are equal

$$\text{i.e.}\ \overrightarrow{i} = F\overrightarrow{K}_c C_A \cdot \exp\left(\frac{-\beta F.\Delta\phi_e}{RT}\right) = \overleftarrow{i} = F\overleftarrow{K}_c C_D \cdot \exp\left[(1-\beta)\cdot F\frac{\Delta\phi_e}{RT}.\right] \ldots\ 2.33$$

The above situation gives rate of two way electron traffic

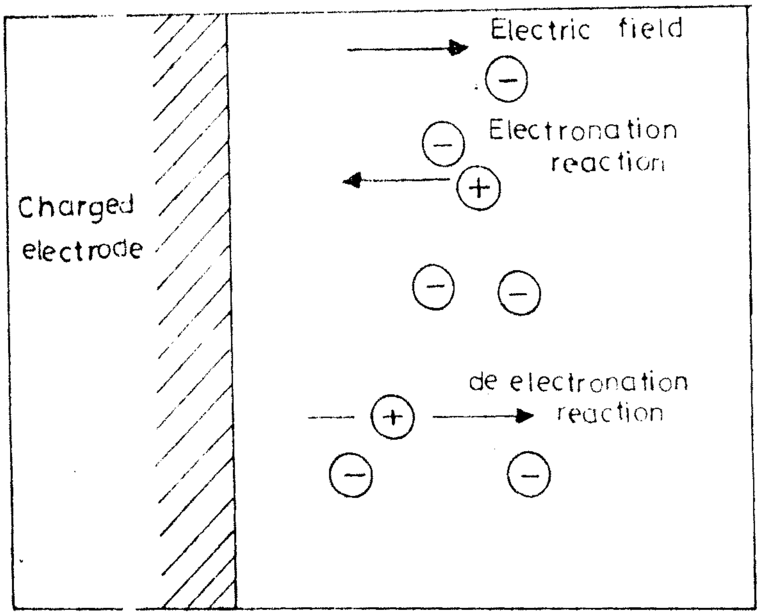

Fig.2.14 (a) Electric field effect on electronation and de-electronation reactions.

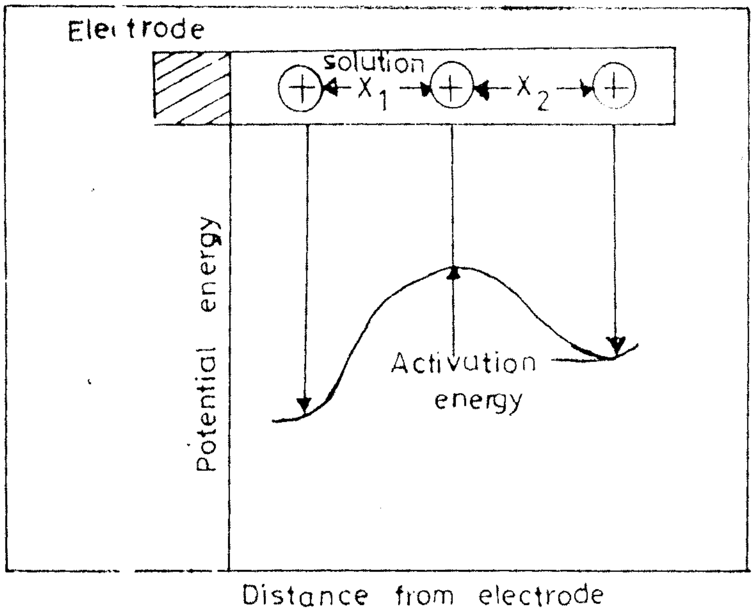

fig.2.14 (b) Contribution of a potential energy distance profile by consideration of the potential energy change produced by varying X_1 and X_2.

between a electrode and an electrolyte when there is no net charge transfer from one phase to the other. The individual current density corresponding to this equilibrium situation is termed as equilibrium current density 'io'. The difference between de-electronation $(\vec{i})$ and electronation $(\overleftarrow{i})$ current densities gives the non-equilibrium current-density (i) given by :

$$i = \overleftarrow{i} - \vec{i} = F\overleftarrow{K}_c C_D \exp\left[\frac{(1-\beta)F\Delta\phi}{RT}\right] - F\vec{K}_c C_A \exp\left[\frac{-\beta F\Delta\phi}{RT}\right] \quad \ldots\ 2.34$$

where , $\Delta\bar{\phi}$ = non equilibrium potential difference across the interface corresponding to the current density i, $(\Delta\bar{\phi} \neq \Delta\phi_e)$. One can split $\underline{\Delta\phi}$ into the equilibrium $(\Delta\phi_e)$ and another portion V, by which the electrode potential departs from the equilibrium,

$$\text{i.e. } V = \Delta\bar{\phi} - \Delta\phi_e \quad \ldots\ 2.35$$

Then we can write the net current density as:

$$i = i_o\left[\exp.(1-\beta)\frac{VF}{RT} - \exp\frac{-\beta VF}{RT}\right] \quad \ldots\ 2.36.$$

Equation (2.36) is called as the famous Butler-Volmer relation |59|, and shows dependence of current density across a metal-solution interface on the portion V. Small changes in V produces large changes in 'i'. An another improtant parameter is symmetry factor 'β'. In the electrode-electrolyte system there is a hill shaped potential barrier even in the absence of electric field as shown in fig. 2.14(b)

|59|. This barrier has to do with the atomic movements in bond stretching which is pre-requisite for processes such as chemical reaction and diffusion of atoms and ions. Electric field modifies the existing potential barrier. The modification is such that only fraction $(1 - \beta)$ of the input electrical energy "qV" turns up into the change of activation energy and hence in the rate expression. This is because the atomic movements necessary for the system to reach a barrier peak are only a fraction of total distance over which the potential barrier extends.

2.6.2 Charge -transfer in light :

The photogenerated carriers in the depletion region upon illumination are separated by an electric field at the interface |82|. This process result in a counter field which is maximum at open circuit condition called as V_{oc} . This photovoltage drags electrons from semiconductor, to the counter electrode , whereas, electrolyte captures the holes. The reaction as a hole can be formulated as:

i) $\text{Red}_{(Solv)} + h^{+} + \rightleftharpoons \text{OX}_{(Solv)}$ ------ (At semiconductor electrode)

ii) $\text{OX}_{(Solv)} + e^{-} \rightleftharpoons \text{Red}_{(Solv)}$ ------- (At counter electrode).

The electrode plays nothing in the reaction but acts only as a shuttle for charge transfer mechanism. Consider a n-type semiconductor in contact with an electrolyte under illumination and let us assume that a forward Voltage 'V' is applied. The schematic showing the energy level diagram of electron is shown in fig. 2.15 (a). The quasi-Fermi levels for electron (E_{Fn}) and for holes (E_{Fp}) in the depletion region are assumed flat. It is further assumed that under forward bias condition the separation between E_{FN} and E_{FP} in the depletion region is 'U' rather than 'V' and is |84|:

$$E_{Fn} - E_{Fp} = qU \qquad \ldots 2.37$$

The assumption that, $U > V$, represents the fact that the minority carrier concentration under light is larger than its concentration in dark. For holes to flow from the semiconductor to electrolyte, U is defined from the reaction ;

$$\exp\frac{(qU)}{KT} = p(W)/p_o \qquad \ldots 2.38$$

where, $p(W)$ = hole concentration at the edge of the depletion region ($x=W$) and P_o = the hole concentration in the bulk of semiconductor in dark at equilibrium. It is assumed that most of the applied voltage appears across the semiconductor depletion region, thus the series resistance of a cell is negligible and electrolyte concentration is high enough such that C_H is atleast a magnitude greater than C_{sc}. From the depletion layer approximation, the width of the depletion layer is :

$$W = Wo\,(V_D - V_o)^{1/2}$$

$$\text{where, } Wo = \frac{(2\epsilon_s\epsilon_0)}{q \cdot N_D}$$

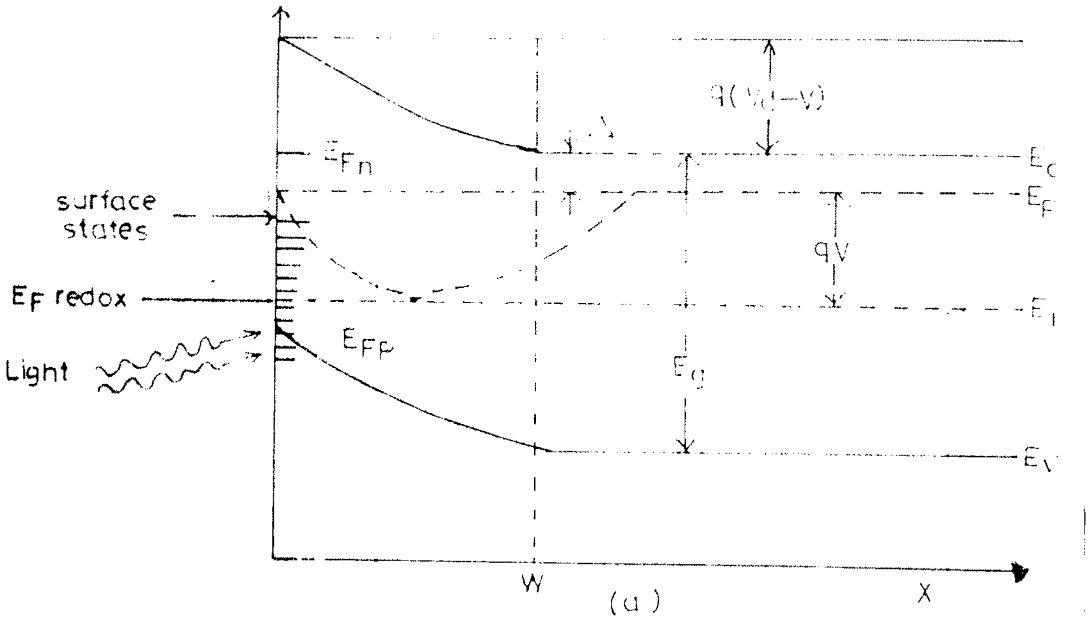

(a)

Fig.2.15(a) Electron energy level diagram for an n-type semiconductor photoelectrode near the S/E interface under illumination and a forward bias V reducing the band bending from qV_D to $q(V_D-V)$.

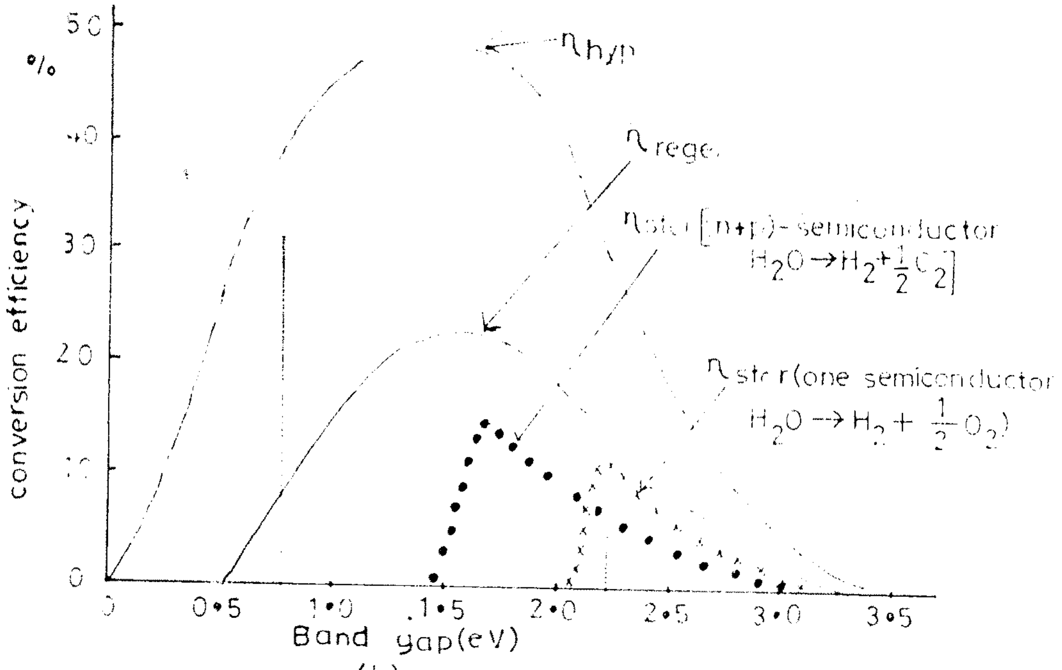

(b)

Fig.2.15(b) Estimated optical conversion efficiencies of the PEC solar cells for power generation (regenerative cell), η_{regen} and storage, η_{stro}. η_{hup} is the theoretical energy conversion effciency for AM_1 (Gerischer-1979).

ϵ_s is a dielectric constant of the material and ϵ_0 is permitivity of a free space , N_D = donor concentration and V_D= equilibrium band bending voltage. The hole flux from depletion region into the cuasi-neutral region at x = W, is |85|.

$$j(W) = D_p \frac{(W)}{L} - \mathring{j}p_0 - \left[\alpha L - \not{\Phi}_0/(1+\alpha L)\right] \cdot e^{-\alpha W} \quad \ldots\ 2.39$$

where , Dp = hole diffusivity,

$L = (D\tau)^{1/2}$ = deffusion length,

τ = hole life time in the bulk of the semiconductor,

$j_{P_0} = D\frac{p_0}{L}$ = reverse saturation flux due to the hole diffusion,

α = light absorption coefficient and

$\not{\Phi}_0$ = incident photon flux after allowing for losses due to reflection and absorption by the electrolyte. At the interface the hole flux into semiconductor is :

$$\dot{j}_{(0)} = \left[\frac{D_p(W)}{L}\right]\left\{1 + \beta \cdot \exp\left(\frac{-qV}{2KT}\right) - \mathring{j}p_0 - \mathring{j}_1(0)\right\} \quad \ldots\ 2.40.$$

Where, $$\beta = \frac{C}{\left[(E_g - qU/2) - \Delta\right]^{1/2}} \quad \ldots\ 2.41.$$

$$C = \frac{\pi k T}{8\sqrt{q}}\left(\frac{\tau}{\tau_t}\right)\left(\frac{\alpha W_0}{\alpha L}\right)\exp.\left[\frac{E_g/2 - \Delta}{K.T}\right] \quad \ldots\ 2.42.$$

$$\tau_t = \frac{1}{6\vartheta^{th}.N_t} \quad \ldots\ 2.43.$$

$$\mathring{j}_1(0) = \Phi_0\left[1 - \frac{\exp(-\alpha W)}{1+\alpha L}\right] \quad \ldots\ 2.44.$$

Where, Eg = Band gap of the semiconductor,

Δ = separation between semiconductor Fermi level in the bulk and the bottom of the conduction band,

6 = capture cross section of electron or of hole for trap density N_t with energy level at or near the intrinsic Fermi level (E_{Fi}) and ν^{th} = carrier thermal velocity ,

$2\tau_t$ = hole effective life time in the depletion region.

At the semiconductor electrolyte interface the holeflux can be described by :

$$j_{(0)} = -(S_t + S_r)\ [\ P_{(0)} - P_{do}\ ] \quad \ldots\ 2.45$$

where , S_t = surface transfer velocity,

S_r = surface recombination velocity and

P_{do} = surface concentration of holes in the dark at equilibrium. S_r depends upon concentration of majority and minority carriers at the surface. The hole flux which contributes to the current is :

$$j = j_{(0)} \cdot \frac{S_t}{S_r + S_t} \quad \ldots\ 2.46.$$

To evaluate equation (2.46), the ratio of the hole density at the surface to hole density at the edge of the depletion region has to be found out from :

$$P_{(x)} = n_i \exp\left[\frac{E_{Fi}(x) - E_{Fp}(x)}{KT}\right] \quad \ldots\ 2.47.$$

one can write:

$$\frac{P_{do}}{P_o} = \exp\left[-qV_D/KT\right] \quad \ldots\ 2.48.$$

$$\frac{p(0)}{p(W)} = \exp\cdot\left[\frac{q}{kT}(V_D - V)\right] \qquad \ldots\ 2.49.$$

where , n_i = intrinsic concentration of semiconductor.

Using (2.38) , (2.40) and (2.45 - 2.49) one obtains :

$$j = j_d - j_t \qquad \ldots\ 2.50.$$

where, j_d = minority carrier flux due to hole injection diffusion and is as :

$$j_d = \left(\frac{S_t}{S_r}\right) jp_0 \left[\exp\left(\frac{qV}{kT}\right) + B \exp\cdot q\left(\frac{V-U}{kT}\right)\right] \qquad \ldots\ 2.51.$$

The direction of 'J_d' is opposite to the photogenerated flux and hence it can be referred to as the opposing flux.

$$j_1 = \left(\frac{S_t}{S_r}\right) \phi_0 \left[1 - \exp\frac{(\alpha - W)}{1 + \alpha t}\right] \qquad \ldots\ 2.52.$$

is the photoflux , which is the useful photogenerated current of a solar cell. The direction of this photocurrent is from semiconductor to the electrolyte. The diode current shown by the equation (2.51) flows in opposite direction to that of the photocurrent and is a combination of three current components |83,85|, namely hole injection current , recombination generation current and electron exchange current. Usually electron exchange component is orders of magnitude greater than the other two. The reasons behind are; i) the concentration of electrons at the surface is much larger than that of the holes and ii) for n - type semiconductor the overlap between the conduction band and oxidised spacies of an electrolyte is greater than the overlap between the valance band and reduced species.

2.7 Some Useful Definitions .

The output voltage/power is mostly limited by the band bending at the interface and a maximum photopotential is obtained at the flat band situation , under high light intensity.

The maximum photopotential is:

$$(V_{ph})_{max} = E_g/q \qquad \ldots\ 2.53.$$

The efficiency of conversion of a cell (η) is defined as:

$$\eta = \frac{(\text{output power})}{(\text{Input power})} \times 100\% \qquad \ldots\ 2.54.$$

The quantum efficiency is defined as:

$$\eta_q = \frac{\text{Numbers of photoelectrons flowing per unit area}}{\text{Number of incident photons with energy } h\nu \text{ per unit area}}$$

$$\eta_q = \frac{N(e)}{N(h\nu)} \qquad \ldots\ 2.55.$$

The various expressions for efficiency used by different authors are manifestation of equations (2.54) and (2.55). Lofersky |86| and Archer |87|, neglecting the losses due to ohmic resistance , overpotential , light absorption in the solution etc., have discussed the efficiency of a photovoltaic cell as :

$$\eta = E_g \int_{E_g}^{\infty} \frac{\alpha(E) N(E) dE}{\int_0^{\infty} E \cdot N(E) dE} \qquad \ldots\ 2.56.$$

where , E_g= band gap of the material ,

$N(E)$ = Number of photons with energy E,

$\alpha(E)$ = Fraction of photons absorbed.

The lower limit in the integral at the numerator (E_g) is the threshold optical energy of the photons responsible for photogeneration of e-h pairs. Equation (2.56) is suggested for the larger magnitudes of band gap (E_g) and α . Further $\alpha(E)$ near the band edge is approximated as :

$$\alpha = \frac{A(h\nu - E_g)^n}{h\nu} \qquad \ldots 2.57.$$

where A is constant and n=1 for direct allowed transitions and n=4 for indirect transition. It is obvious from equation (2.57),that for 'α' to be large, E_g must be small. Thus equations (2.56) and (2.57) are the two conradictory conditions and 'η' would be a maximum for some optimum value of E_g . Assume that all the photons are absorbed in a narrow region beneath the interface (α= 1). Neglecting all possible losses, the hypothetical conversion efficiency, η , can be given as :

$$\eta_{hyp} = E_g \int_{E_g}^{\infty} \frac{N(E)dE}{\int_0^{\infty} E\cdot N(E)\cdot dE} \qquad \ldots 2.58.$$

A simple calculation for AM_1 solar radiation is given in fig.2.15(b). The conversion efficiency has a maximum around E_g = 1.2eV, with the maximum value 47%. For real conversion efficiency, the following losses are to be considered |80|:

i) Ohmic loss across the external load iR_L,

ii) Energy lost in the separation of e-h pair in the space charge layer.

iii) Losses due to minority carriers ($q\eta'_{min}$) and majority carriers ($q\eta'_{maj}$) at the semiconductor and counter electrodes respectively. The estimated loss of energy is approximately,

$$\Delta G_{loss} \geqslant 0.5 + e(\eta'_{min} + \eta'_{maj}) + iR_L \quad \ldots\ 2.59.$$

The real situation conversion efficiency as a function of the bandgap for regenerative type electrochemical photovoltaic cell is given as :

$$\eta'_{regn} = \eta_{hyp}(1 - \Delta G_{loss}/E_g) \quad \ldots\ 2.60.$$

On the similar lines of equation (2.54), the efficiency of an externally biased cell can be defined as |25| :

$$\eta' = \frac{\text{(output-chemical power)} - \text{(electrical input power)}}{\text{input optical power}} \quad \ldots\ 2.61.$$

Account for ohmic loss in the external load can be |88|,

$$\eta'' = \frac{i^2 R_L + i\,Q_{H_2}/2F}{W_{ph}} \quad \ldots\ 2.62.$$

where QH_2 = heat of combustion of H_2 (68.k.cal.mol) or (285.6 k.J.mol),

F = Faraday constant,

i = Photocurrent flowing though R_L and

W_{ph} = incident light energy,

For storage devices, the storage efficiency is :

$$\eta_{stor} = \eta_{h\gamma P}(1 - \Delta E_{stor}/E_g) \quad \ldots 2.63.$$

where $\Delta E_{stor} \leq E_g - \Delta G_{loss}$, otherwise storage would not take place ΔE_{stor} = equilibrium cell voltage of the H_2 / O_2 fuel cell in the case of water photoelectrolysis. From fig. 2.15(b), it is clear that a theoretical efficiency of about 25% is expected for regenerative type PEC cells for a semiconductor with E_g = 1.4 to 1.7 eV. The band gap of some of the semiconductors vis-a-vis efficiency is given in fig. 2.16(a).

The conversion efficiency for photoelectrolysis cell with single electrode is much lower about 12% with a semiconductor of optimum bandgap of about 2.2eV. Much lower bandgap semiconductors can, however, be used in photoelectrolysis cell with two (n + p) electrode combination. Now it is well known that the maximum open circuit voltage attainable from an electrochemical photovolatic cell would be :

$$V_{OC} = V_{Redox} - V_{fb} \quad \ldots 2.64.$$

Thus, the ultimate efficiency would also depend upon $V_{Redox} - V_{fb}$ as shown in fig. 2.16(b).

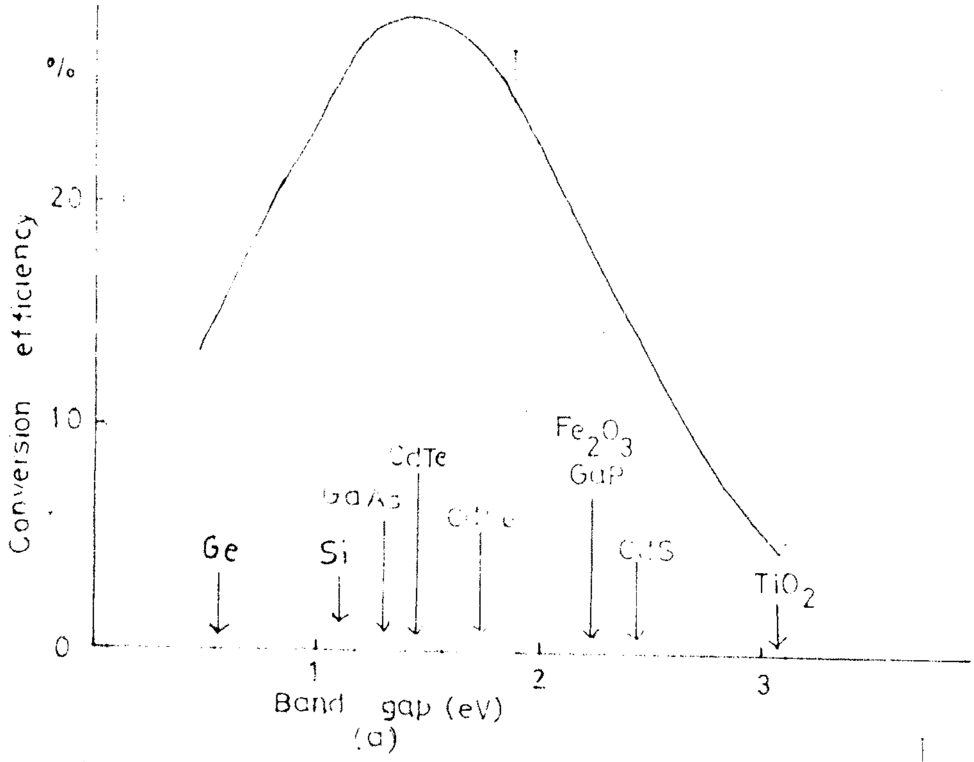

Fig.2.16(a) The predicted conversion efficiency for of PEC's as a function of band gap for AM$_1$.

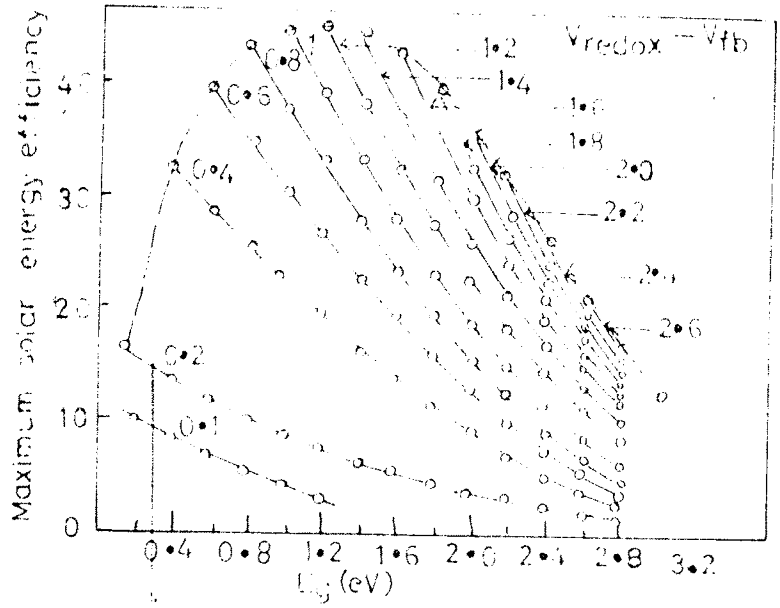

fig.2.16(b) Maximum solar energy conversion efficiencies for open circuit solar cells with various values of E_g and $(V_{redox} - V_{fb})$, (Noufi and Warreen 1980).